IDŐJÁRÁS

QUARTERLY JOURNAL
OF THE HUNGARIAN METEOROLOGICAL SERVICE

CONTENTS

****

http://www.met.hu/firat/ido-e.html

VOL. 105 * NO. 1 * JANUARY–MARCH 2001

IDŐJÁRÁS

Quarterly Journal of the Hungarian Meteorological Service

Editorial Office: P.O. Box 39, H-1675 Budapest, Hungary or
Gilice tér 39, H-1181 Budapest, Hungary
E-mail: prager.t@met.hu or *antal.e@met.hu*
Fax: (36-1) 346-4809

Subscription by

mail: IDŐJÁRÁS, P.O. Box 39, H-1675 Budapest, Hungary
E-mail: prager.t@met.hu or *antal.e@met.hu*; *Fax: (36-1) 346-4809*

IDŐJÁRÁS

Quarterly Journal of the Hungarian Meteorological Service
Vol. 105, No. 1, January–March 2001, pp. 1–17

Regional climate change in Hungary: a survey and a stochastic downscaling method

Judit Bartholy, István Matyasovszky and **Tamás Weidinger**

Department of Meteorology, Eötvös Loránd University,
H-1518 Budapest, P.O. Box 32, Hungary; E-mail: bari@ludens.elte.hu

(Manuscript received 2 June 2000; in final form 27 December 2000)

Abstract—The first part of this review paper summarizes the changes in Hungarian temperature and precipitation series during this century. Then, some possible hydrological, agricultural and ecological consequences of a future climate change are outlined, obtained after using empirical downscaling techniques developed for estimation of local effects of a global climate change. Finally, local temperature and precipitation changes corresponding to the doubling of the concentration of atmospheric greenhouse gases obtained with a stochastic downscaling method are presented. Climate of Hungary has become warmer and dryer during this century. The global climate change expected under increasing concentration of atmospheric greenhouse gases further contributes to this tendency.

Key-words: regional climate change, downscaling, stochastic model, temperature, precipitation.

1. Introduction

A presumably global climate change due to the increasing concentration of atmospheric greenhouse gases is an important issue for many reasons. Local consequences of this global change may be quite variable over different regions of even a relatively small area.

In order to simulate climates, atmospheric and coupled atmosphere-ocean general circulation models (GCMs) are widely used. A standard method to assess the change of climate mainly on the atmospheric GCMs (AGCM) is to run such a model under atmospheric CO_2 concentration before the industrial revolution ($1\times CO_2$ case) and, then, run it again under doubled CO_2 content ($2\times CO_2$ case). For coupled models a modified version of the $2\times CO_2$ experiment is to run the ocean-atmosphere model from the present or previous climate under continuously increasing CO_2 concentration, until it reaches the doubling level. This non-equilibrium, but more realistic state (say 10 years averages) is

compared to initial state. However, due to the relatively low horizontal resolution (a few hundred kilometers for the coupled and about one hundred for the equilibrium AGCMs) and quite simple parameterizations of these models (atmosphere-surface feedbacks, radiative processes, cloud and precipitation forming, etc.), the results for small areas, such as the Carpathian Basin, are considerably uncertain. There is a need, therefore, to "downscale" the large-scale output of GCMs to smaller scales.

There are three main types of downscaling approaches (*Giorgi* and *Mearns*, 1991). The basis of empirical techniques is a quite strong assumption that similar large-scale climate changes have similar local consequences independent of the factors causing the global change. This hypothesis motivates the use of temporal or spatial analogies (*Mika*, 1992; *Rácz*, 1999).

Another type of downscaling methods include meso-scale numerical modeling. Meso-scale models use GCM outputs as initial and boundary conditions (*Giorgi et al.*, 1992; *Marinucci et al.*, 1995; *McGregor*, 1997). This technique requires substantial effort in terms of modeling and computer programming and no satisfactory long simulation is available to assess extremes. These difficulties, among others, may motivate the use of stochastic downscaling procedures which appear to be specific combinations of the previous two techniques.

Stochastic downscaling methods have two key elements. The first element includes large-scale circulation of the atmosphere and the second element represents a linkage between local surface variables and large-scale circulation. The linkage is expressed by a stochastic model using an observational data series. Then, this model may be utilized with GCM outputs characterizing atmospheric circulation (*Bogárdi et al.*, 1993; *Bartholy et al.*, 1995a; *Giorgi et al.*, 1999).

Examination of local effects of climate change started at the end of eighties in Hungary. Climate change scenarios have been created for Hungary by *Mika* (1988, 1991, 1992) using an empirical downscaling method and, later, for smaller and sensitive regions of the country, namely for the watershed of Balaton-Sió and the Great Hungarian Plain (*Fig. 1*) by *Bartholy et al.* (1995b), *Bartholy* and *Matyasovszky* (1998) based on a stochastic downscaling technique. Causes and magnitude of climate change, as well as its hydrological, agricultural, forestrial and energetic consequences were evaluated (*Faragó et al.*, 1990, 1991; *Faragó*, 1998). Recently, transformation of the land of the Great Hungarian Plain is analyzed as a consequence of changing climate (*Mika et al.*, 1995; *Kertész et al.*, 1999).

The first part of the present review paper summarizes trend analyzes of the long time series of annual mean temperature and annual precipitation amount. Then, major results obtained from an empirical downscaling technique are presented. In the next section, a stochastic downscaling method and its results are discussed. Finally, a brief section for summary is provided.

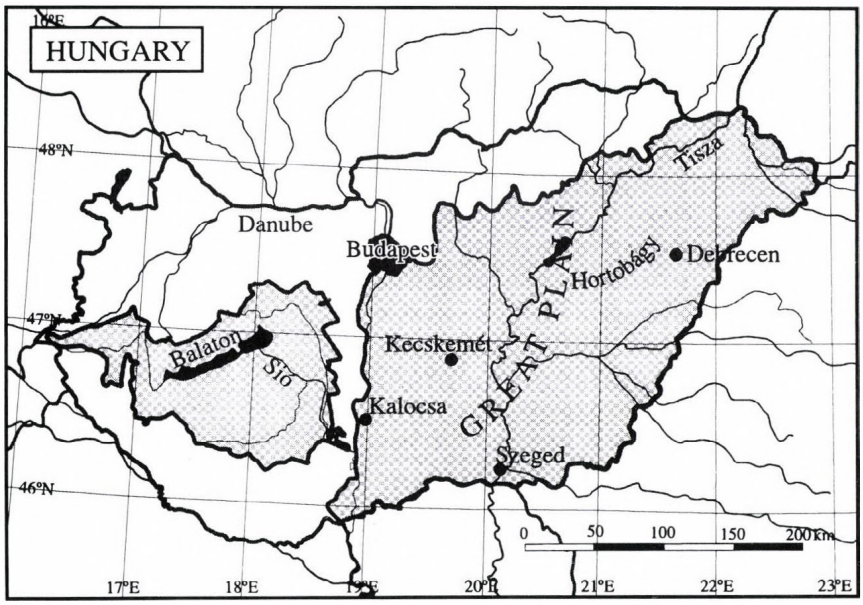

Fig. 1. The two sensitive regions of Hungary selected for the stochastic downscaling model.

2. Trends of temperature and precipitation in Hungary

Hungary is located in the middle of Carpathian Basin (Fig. 1) with a climate formed by oceanic, continental and slightly Mediterranean influences. Spatial distribution of temperature is principally driven by latitude. Maximum values (11–11.5 °C) are found in the southeastern margins of the country, but hilly northern regions have only 8–9 °C annual mean temperatures. The coldest month is January with –1– –4 °C mean temperatures, while the warmest period can be identified by month July, when the mean temperature is between 18–22 °C.

The mean annual precipitation amount is about 550–600 mm. Maximum values (800–900 mm) appear at the southwestern margins of the country; the lowest amounts (below 500 mm) are measured in Hortobágy (see Fig. 1) and in southeast of the country. Precipitation also has a characteristic annual cycle. Largest amounts are detected at the beginning of summer (June), the smallest ones in the second part of winter. In the southwestern region, there is a small second maximum of precipitation amounts due to Mediterranean effects in the period October-November. Precipitation is a highly variable meteorological element in Hungary as in many areas of the Earth. The ever observed wettest years gain three times more precipitation than the driest ones, and each month may suffer total shortage of precipitation (*Péczely*, 1981).

Molnár and *Mika* (1997) performed a linear trend analysis of temperature and precipitation for 16 locations in Hungary using homogenized time series for the period from 1881 to 1990. The methodology of homogenization is described by *Szentimrey* (1995, 1996). Each station exhibits a warming tendency at least at a 5% significance level with an average rate of 1 °C/100 year. Variation of the rate of increasing temperature is quite small and is in good agreement with other results for Central Europe (*Brazdil*, 1992; *Böhm*, 1992).

Daily maximum and minimum temperatures have also been examined for five locations in Hungary for this century. *Iványi* (1995) and *Domonkos* (1998) concluded that these data are characterized by decadal fluctuations rather than long-term changes.

Precipitation shows a negative trend, which is statistically significant at a 5% level for 10 stations. The average rate of the change is –90 mm/100 year with a largest value of –230 mm/100 year and a smallest one of –27 mm/100 year. A previous work (*Koflanovits-Adámy* and *Szentimrey*, 1986) performed for 84 stations in the Carpathian Basin for the period from 1901 to 1984 resulted in similar results. Aridification of this region is confirmed by *Bartholy* and *Pongrácz* (1998). *Tar* (1992) and *Molnár* (1996a; 1996b; 1996c) analyzed the frequency of years warmer or colder than average as well as dryer or wetter years as compared to the average. They found a statistically significant increasing trend of warm and dry years.

3. Effects of climate change in Hungary obtained from empirical downscaling methods

Climate change analyses generally concentrate on temperature and precipitation, and the performance of several other meteorological elements can be estimated using the changes of the two above parameters. An estimation of the climate for Hungary or for the total Carpathian Basin under changing global climate was performed by *Mika* (1988, 1991, 1992) and *Molnár* and *Mika* (1997) using: (i) a statistical relationship between local meteorological elements and Northern Hemisphere temperature and ocean-continent temperature contrast; (ii) paleoclimatological analogies; (iii) a simple regional energy balance model. Results for changes of regional climate as a function of the change of average hemisphere temperature are summarized in *Table 1*. As it is expected, the largest the hemisphere temperature change, the largest the local response. However, behavior of precipitation is non-linear. A small global warming (0.5–1 °C) results in a considerable dryer climate, but a 4 °C warmer Northern Hemisphere yields much wetter local climate. Also, wide range of estimated changes indicates high uncertainty. A moderate global warming

entails a 20% increase of sunshine duration and the average duration of drought periods from the actual value of 1.4 month/year to 2 month/year.

Table 1. Expected changes of temperature and precipitation in Hungary, in connection with different values of hemispheric temperature changes after *Molnár* and *Mika* (1997). Calculation of the annual mean temperature changes is added by the authors. (Intervals indicate high uncertainty.)

Hemispheric temperature change ΔT, [°C]	**+0.5**	**+1**	**+2**	**+4**
Temperature change for Hungary, summer*	+0.6	+0.8	+1.5	+3
Temperature change for Hungary, winter*	+0.1; +0.5	+1 ; +2.5	+3	+6
Temperature change for Hungary, year	+0.3; +0.6	+0.9; +1.6	+2; +2.5	+4; +5
Precipitation change for Hungary, year, [mm]	–30	–20; –100	+ or 0	+40; +400
Geographical analogy	within HU; Voyvodina, YU Zhil-valley, RO; Plovdiv, BG	Varna, BG	Burgas, BG Yalta, UKR	Firenze, I; Washington, U.S.A.

* The +0.5°C column refers to the summer and winter half years.

These changes of temperature and precipitation can produce several ecological, agricultural and economical problems. Ecological effects include —for instance—drought, drying of upper layer of soils, sinking of ground water level, which arise problems of demand for increasing irrigation and, thus for more reservoirs. Such possible dangers especially affect large lowland areas between the Danube-Tisza Interfluve, where sinking of the ground water level has started in the middle of seventies (*Kertész et al.*, 1999) and partly recovered just in the recent normal and wet years.

As a consequence of change of climate and soil conditions it is important to evaluate crop outlooks. For instance, crop of maize and wheat was examined and a 10–20% decrease was obtained, which, however, can be partly compensated by the increasing atmospheric CO_2 concentration, milder winters and modest denitrification due to the dryer climate (*Bacsi* and *Hunkár*, 1994; *Harnos*, 1998; *Kovács* and *Dunkel*, 1998). Relationship between climate change and possibilities of plant migration was analyzed by *Mátyás* (1997) and *Kovács et al.* (1998).

4. Local effects of climate change in Hungary obtained from a stochastic downscaling model

Stochastic downscaling methods are based on the fact that there exists a considerable stochastic relationship between large-scale atmospheric circulation and meteorological, hydrological (hydrometeorological) variables. Frequently, the large-scale circulation pattern (CP) is classified and every day is assigned to one of daily CP types. The relationship is estimated from observed data and then is used with large-scale circulation available from GCM output for present climate ($1\times CO_2$) and $2\times CO_2$ cases. Thus, an estimation can be obtained for local hydrometeorological parameters under a new, such as $2\times CO_2$ climate (*Bogárdi et al.*, 1993). Such a methodology is based on two assumptions. The first part assumes that the GCM-produced CP types may be considered the same as the types obtained from observed data. This part of the hypothesis can be verified. The other part of the hypothesis assumes that if observed data reflect a linkage between daily CP types and daily local hydrometeorological factors, this linkage will remain in a climate change situation. This part of the hypothesis cannot be checked with statistical means and probably is not fully valid because of the direct change of the radiation balance and the corresponding surface-biosphere-atmosphere feedbacks. These latter interactions, however, are known relatively inaccurately and it is difficult, even if at all possible, to predict how such a linkage may change. Changes of the radiative balance could, however, be estimated by a locally adjusted radiative-convective model (*Práger* and *Kovács*, 1988). Without these effects, the results of downscaling represent a partial approach of the full (i.e., radiative plus advective) change of the thermal variables.

The methodology consists of three main parts. First, a system of large-scale circulation patterns is defined using the spatial distribution of either sea level air pressure, or middle tropospheric pressure heights. One of the main approaches to classify such spatial variables includes subjective classifications when meteorological experience is applied. These classifications are subjective because they reflect the attitudes of meteorologists, but are objective in the sense that are based on the physical behavior of the atmosphere. For instance, the so-called Hess-Brezowsky system of circulation types (*Hess* and *Brezowsky*, 1969) is frequently used in Europe for many purposes. Another classification approach consists of objective classification methods. Objectivity means here that a given algorithm automates the data processing, although the choice and application of a given algorithm is subjective. This type of classification is generally based on different versions of clustering (*Wilson et al.*, 1992), fuzzy clustering (*Bárdossy et al.*, 1995), classification using neural networks (*Muster et al.*, 1994), or other techniques (*Breinman et al.*, 1984).

In the second step of the methodology a stochastic model is developed to describe the behavior of hydrometeorological variables as conditioned on circulation types. In order to reproduce the space-time statistical structure of local hydrometeorological variables, a suitable model should be chosen. Autoregressive processes represent a well-developed and commonly used tool to model time series. They have been developed principally for Gaussian processes, but climatic factors do not usually follow a Gaussian distribution. Therefore, it is desirable to construct a transformation establishing a relationship between the distribution of a local climatic factor and a normal distribution.

Let the vector $\mathbf{Z}(t) = (\mathbf{Z}(t,u_1), \mathbf{Z}(t,u_2), \ldots, \mathbf{Z}(t,u_K))$ represent a daily climatic variable at locations $u_1, u_2, \ldots, u_K$ and time t and let $\mathbf{W}(t)$ be a K-dimensional normal random vector at time t. We suppose for simplicity that each component of the vector $\mathbf{W}(t)$ has zero mean and unit variance. For a fixed CP type and time t, any component Z of $\mathbf{Z}(t)$ can be related to the corresponding component W of $\mathbf{W}(t)$ prescribing that

$$P(Z<z) = F(z) = p, \tag{1}$$
$$P(W<w) = \Phi(w) = p, \tag{2}$$

where Φ is the standard normal distribution function and p is any value satisfying $0 < p < 1$ for temperature and $p_0 < p < 1$ for precipitation, p_0 being the probability of precipitation occurrence. Thus:

$$Z = F^{-1}(\Phi(W)). \tag{3}$$

Estimating $F(z)$ is a simple task for temperature, since the temperature is distributed nearly normally. For the purpose *Matyasovszky et al.* (1994a) used binormal distributions (*Tóth* and *Szentimrey*, 1990). Precipitation, however, represents a much more complicated task. Namely, the probability distribution function of daily precipitation can not be considered as continuous due to dry days, i.e., $F(z)$ has a form:

$$F(z) = \begin{cases} 0, & z < 0 \\ (1-p_0) + p_0 H(z), & z \geq 0 \end{cases},$$

where H is the probability distribution function of daily precipitation amount on wet days. In order to model $F(z)$, *Bárdossy* and *Plate* (1992) proposed a power transformed truncated normal distribution which, however, does not work under the climate of Hungary. Therefore, *Matyasovszky et al.* (1993) developed a non-parametric technique to estimate distribution function of daily precipitation.

The time dependency of $\mathbf{W}(t)$ is described using first order autoregressive ($AR(1)$) processes. The transformation of the random vector $\mathbf{Z}(t)$ into the normal vector $\mathbf{W}(t)$ depends on the climatic variable under consideration. The process $\mathbf{W}(t)$ is described by the following multivariate $AR(1)$ process when CP type j occurs at time t:

$$\mathbf{W}(t) = \mathbf{B}_j \mathbf{W}(t-1) + \mathbf{C}_j \mathbf{U}(t) . \tag{4}$$

Using the so-called Yule-Walker equations, the matrices $\mathbf{B}_j$ and $\mathbf{C}_j$ can be calculated as

$$\mathbf{B}_j = \mathbf{G}_{1j}\mathbf{G}_{0j}^{-1}, \tag{5}$$

$$\mathbf{C}_j\mathbf{C}_j^{T} = \mathbf{G}_{0j} - \mathbf{G}_{1j}\,\mathbf{G}_{0j}^{-1}\mathbf{G}_{1j}^{T} \tag{6}$$

and $\boldsymbol{G}_{0j}$, $\boldsymbol{G}_{1j}$ are the covariance matrices of $\mathbf{W}(t)$ for lags 0 and 1 and CP type j, respectively. $\mathbf{U}(t)$ represents a K-dimensional standard normal vector which consists of K standard normal uncorrelated random variables. The matrices $\mathbf{G}_{0j}$, $\mathbf{G}_{1j}$ can directly be estimated from observed data in the case of temperature due to its nearly normality. However, these matrices can only be estimated indirectly when precipitation is in question. Indicator series defined by precipitation quantiles are used to estimate the correlations among the indicator series; the required correlations can then be calculated from the indicator series correlations. The indicator series $I_Z(t,u_k)$ is defined for any q, $1-p_{0k} < q < 1$ as

$$I_Z(t,u_k) = 1, \quad Z(t,u_k) \geq z_{qk}, \tag{7}$$

$$I_Z(t,u_k) = 0, \quad Z(t,u_k) < z_{qk}, \tag{8}$$

where z_{qk} is the qth quantile of precipitation at location u_k. Indicator series $I_W(t,u_k)$ of W and $I_Z(t,u_k)$ are the same due to the transformation between Z and W. The required correlation $g(i,k)$, the (i,k)th element of $\mathbf{G}_0$, is related to the correlation of the indicator series $g^{(q)}(i,k)$ through the relationship (*Abramowitz* and *Stegun,* 1965, p. 128)

$$g^{(q)}(i,k) = \frac{1}{2\pi(1-q)q} \int_0^{\sin^{-1}(g(i,k))} \exp\left(-\frac{w_q}{1+\sin(s)}\right) ds , \tag{9}$$

where w_q is the qth quantile of standard normal distribution. This equation can be solved for $g(i,k)$ using a numerical algorithm. The elements of $\mathbf{G}_1$ are derived in a similar way.

In the final step, statistical characteristics of four time series are compared and thus a local climate change estimation is obtained. The four time series consists of observed data, simulated data corresponding to present climate, and simulated data corresponding to both GCM-generated $1\times CO_2$ and $2\times CO_2$ climates. Simulated data are obtained by the stochastic model with either observed circulation types or circulation types generated by a GCM.

The authors developed and applied such a model to two sensitive regions of the Carpathian Basin (Fig. 1), namely for the watershed of Balaton-Sió (*Bartholy et al.*, 1995b; *Weidinger et al.*, 1994; *Weidinger et al.*, 1995) and the Great Hungarian Plain (*Bartholy* and *Matyasovszky*, 1998) and to several other areas, such as to dry continental climate of Nebraska (*Matyasovszky et al.*, 1993; 1994b), dry subtropics of Arizona (*Bartholy* and *Duckstein*, 1994), the Mediterranean climate of Greece (*Matyasovszky et al.*, 1995) and to Alpine region in Austria (*Nachtnebel et al.*, 1996). Computations were carried out using ECHAM, a coupled GCM developed by Max Planck Institute for Meteorology, Hamburg, Germany (*Cubash et al.*, 1991), and a GCM of Canadian Climate Centre (CCC), Victoria, Canada (*Boer et al.*, 1984). ECHAM shows a 1.5 °C global warming at reaching the non-equilibrium $2\times CO_2$ concentration, while CCC, which does not have a coupled ocean model predicts 3.5 °C global equilibrium temperature increase (*Boer et al.*, 1984). Results presented in *Fig. 2* are based on ECHAM model.

Expected temperatures under $2\times CO_2$ climate have no considerable spatial variability in the Great Hungarian Plain (*Fig. 3*). Each season exhibits a statistically significant positive trend, which is, however, only 0.1–0.5 °C except for autumn where the increase of temperature exceeds 1.5 °C (*Bartholy* and *Matyasovszky*, 1998). Thus the annual mean temperature change is about +0.7 °C, which is considerably smaller than the global warming 1.5 °C produced by the ECHAM, and corresponding values in Table 1 (after *Molnár* and *Mika*, 1997). *Fig. 4*, showing the probability density function of daily mean temperature in Kecskemét for October, demonstrates that not only the means but also the standard deviations will change under the non-equilibrium $2\times CO_2$ climate. Decreasing tendency of standard deviations implies a less variability of temperature.

Evaluation of precipitation is a much more complicated task since it has a spatio-temporal intermittence (*Bogárdi et al.*, 1993). Therefore, it is necessary to analyze both the probability of precipitation occurrence and the amount of precipitation during a wet period. Another important characteristic is the probability distribution of wet and dry day durations. A major experience of our examination is that frequency of precipitation occurrence becomes smaller,

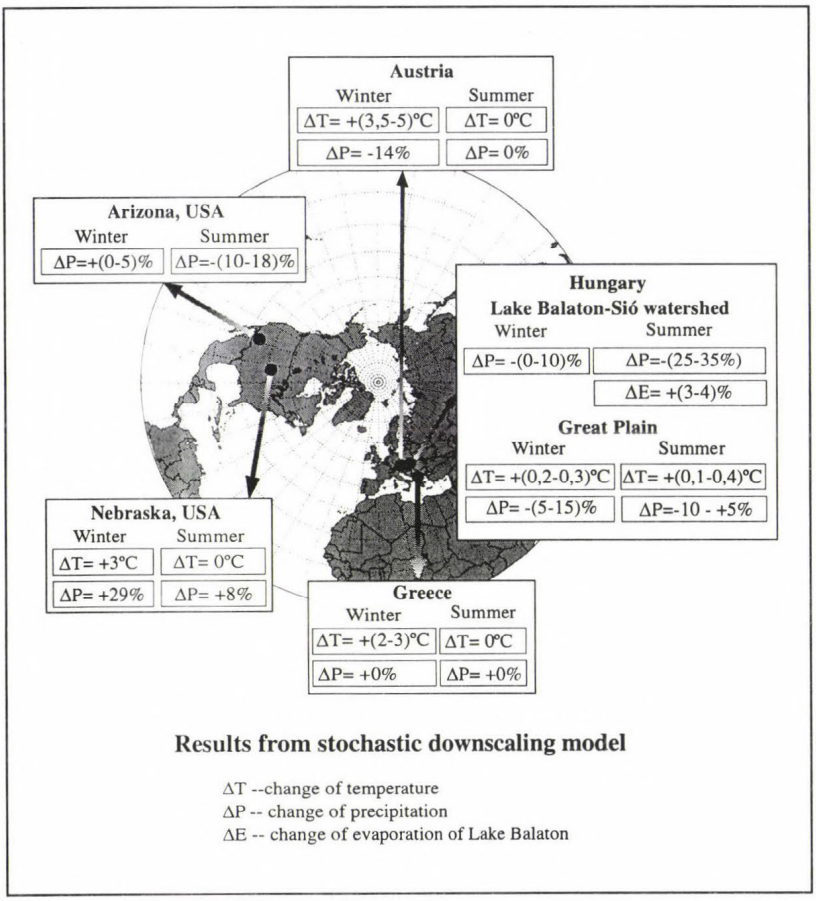

Fig. 2. Regional climate change results from the stochastic downscaling model in different regions of the Northern Hemisphere.

while the amount of precipitation in wet periods seems larger or at least not smaller. This indicates a precipitation climate that is more variable in time (*Matyasovszky et al.*, 1993; *Matyasovszky et al.*, 1995; *Nachtnebel et al.*, 1996). On the other hand, the change of precipitation amounts shows slight spatial differences in the Great Hungarian Plain (*Bartholy* and *Matyasovszky*, 1998). In summer (*Fig. 5*), precipitation amount slightly decreases with a rate of +5 – –10%, while the winter has a more characteristic decreasing tendency by –5 – –15%. Summarizing each season, the change of annual precipitation is slightly below 10%.

The same analysis was carried out for the watershed Balaton-Sió by using 28 precipitation stations (*Bartholy et al.*, 1995). Both the frequency and the

amount of precipitation in wet days decrease substantially in summer. Spatial distribution of precipitation is slightly more complicated in winter. Frequency of precipitation occurrence is surely decreasing, but the amount on wet days is decreasing (increasing) over a larger northern (a smaller southern) part of the area, respectively. Finally, the precipitation amount appears to have a 25–35% decrease in summer, while the winter will probably have only a slightly dryer (0–10% decrease) climate.

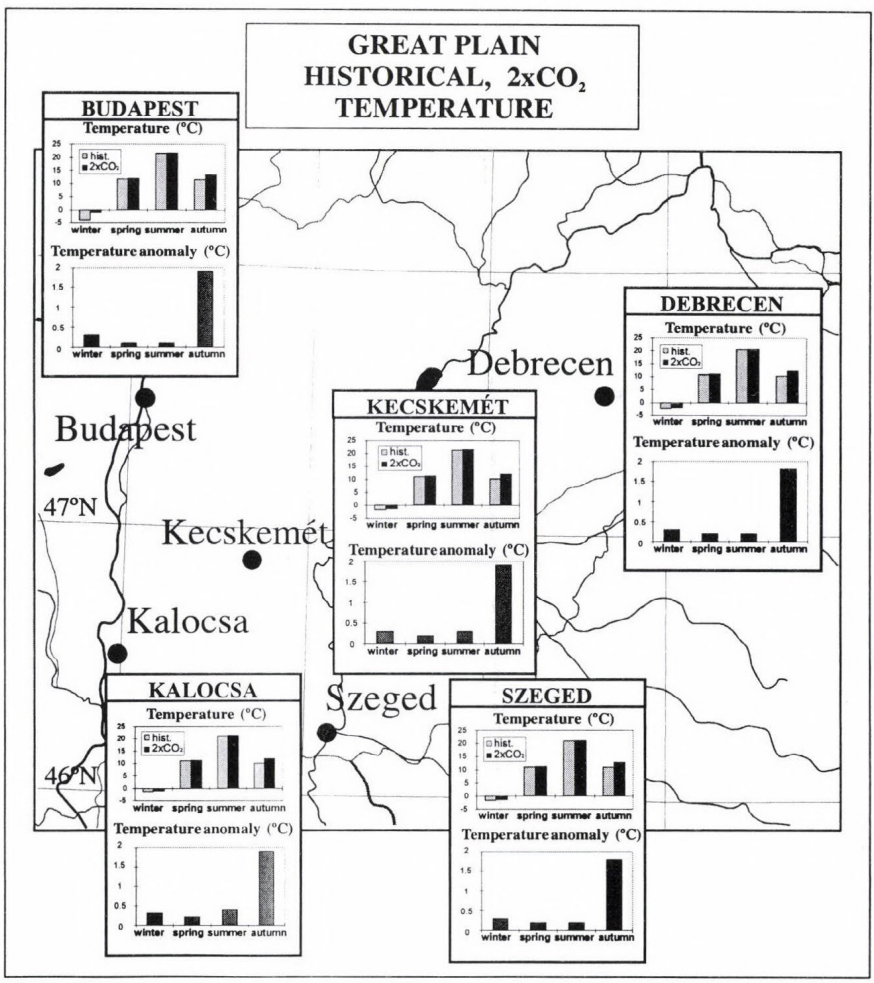

Fig. 3. Expected changes of temperature for selected stations in the Great Hungarian Plain obtained from a stochastic downscaling technique with doubled atmospheric CO_2 concentration.

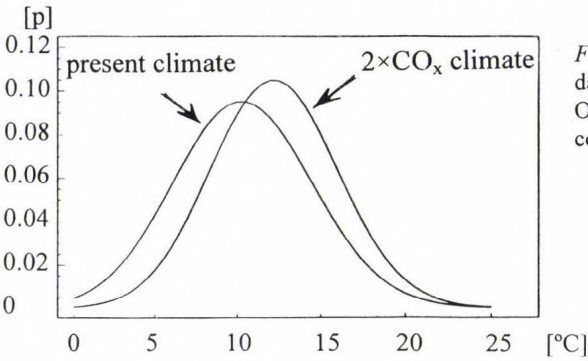

Fig. 4. Probability density functions of daily mean temperature in Kecskemét for October under present and 2×CO_2 climate conditions.

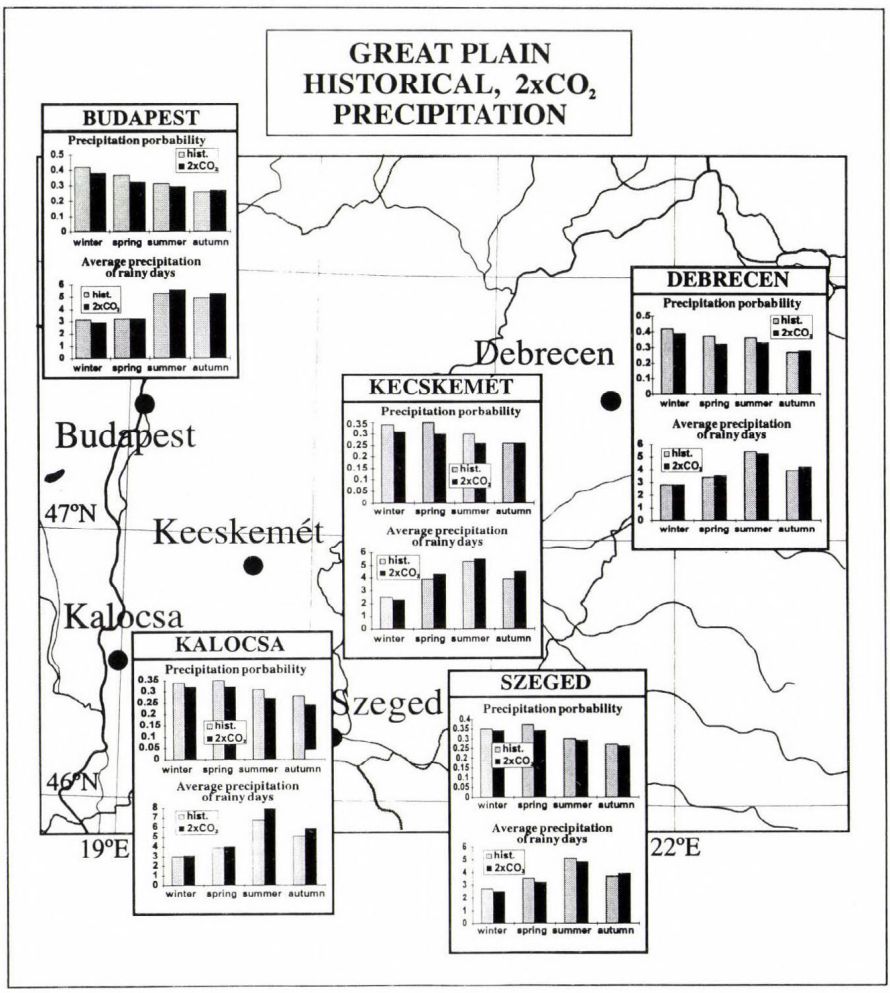

Fig. 5. Expected changes of precipitation for selected stations in the Great Hungarian Plain obtained from a stochastic downscaling technique with doubled atmospheric CO_2 concentration.

Smaller changes of precipitation were obtained for the Great Hungarian Plain, suggesting that smaller differences can be expected within the region in case of a dryer regional climate (*Table 2*).

Table 2. Expected changes of temperature [°C] and precipitation [mm] in Hungary, obtained with a stochastic downscaling technique for doubled atmospheric CO_2 concentration

Hemispheric temperature change ΔT, [°C]	**+1.5**
Temperature change for the Great Hungarian Plain, summer	+0.2 ; +0.3
Temperature change for the Great Hungarian Plain, winter	+0.1 ; +0.4
Temperature change for the Great Hungarian Plain, year	~ +0.7
Precipitation change for the Great Hungarian Plain, summer [mm]	–20 ; +5
Precipitation change for the Great Hungarian Plain, winter	–20 ; –5
Precipitation change for the Great Hungarian Plain, year	–40 ; +10
Precipitation change for Lake Balaton-Sió watershed in Hungary, summer	–75 ; –35
Precipitation change for Lake Balaton-Sió watershed in Hungary, winter	–15 ; 0

A modified version of our stochastic downscaling methodology was also applied for assessing evaporation of Lake Balaton under $2\times CO_2$ climate. The lake evaporation was estimated by adjusting pan evaporation measurements of surrounding locations (*Weidinger et al.*, 1995). Calculations performed for summer months indicate only a 3–4% increase of evaporation, which is in a good agreement with the slight warming obtained for this season.

5. Summary

Main conclusions of the linear trend analysis for time series of homogenized annual mean temperature and annual precipitation amount in Hungary are summarized in the following few sentences. An increasing trend of annual mean temperature is statistically significant at least at a 95% level and reaches 1 °C/100 year. A decreasing trend of annual precipitation amount is statistically significant at least at a 95% level and reaches 90 mm/100 year. As a consequence of the above two facts, a clear aridification proceded during the 20th century. This tendency will probably be strengthened by the increasing concentration of atmospheric greenhouse gases.

Our stochastic downscaling method for a doubled CO_2 concentration for two sensitive climate regions of Hungary (the Balaton-Sió watershed and the Great Hungarian Plain) has resulted in:

(i) The 0.7 °C increase of annual mean temperature obtained with a stochastic downscaling method under a 1.5 °C global warming (from the ECHAM model) is considerably smaller than the previous estimations. One of the reasons might be the lack of direct radiation effects on temperature, not considered by the method.

(ii) Anticipated temperature changes in Hungary are substantially smaller than changes estimated for other regions of Earth located nearly at the same latitudes as Hungary, given in Section 4. This difference, however, can not be connected to the lack of radiation processes.

(iii) The frequency of wet days is estimated as decreasing for future, while precipitation amount on wet days is expected to be quite variable.

(iv) Future precipitation deficit over the Balaton-Sió watershed seems remarkably greater than in the Great Hungarian Plain. The scale of our climate change scenarios for precipitation is similar to a previous estimation using an empirical downscaling method, but the results obtained for different regions point out the necessity of distinction even within small areas.

Acknowledgements —Research leading to this paper was supported by Finance for High Education and Investigation Projects FKFP-0193, Hungarian Scientific Funds OTKA-T026629, OTKA-T025803 and János Bólyai Research Scholarship. Authors are very grateful for *János Mika* from Hungarian Meteorological Service and two anonymous reviewers for their helpful comments.

References

Abramowitz, M. and *Stegun, I.*, 1965: *Handbook of Mathematical Functions.* Dover Mineola, N. Y.

Bacsi, Zs. and *Hunkár, M.*, 1994: Assessment of the impacts of climate change on yields of winter wheat and maize, using crop models. *Időjárás 98*, 119-134.

Bartholy, J. and *Duckstein, L.*, 1994: Comparing and extending the CCC and MPI GCM outputs from western USA for global change studies. *Annales Gepohysicae, Supplement II. to Vol. 12*, C355.

Bartholy, J., Barcza, Z. and *Matyasovszky I.*, 1995a: Large-scale changes – regional consequences. Methodological study on regional climate change predictions. *Annales Geophysicae, Supplement II. to Vol. 13*, C333.

Bartholy, J., Bogárdi, I. and *Matyasovszky, I.*, 1995b: Effect of climate change on regional precipitation in Lake Balaton watershed. *Theor. Appl. Climatol. 51*, 237-250.

Bartholy, J. and *Matyasovszky, I*, 1998: Effect of climate change on temperature and precipitation in the Carpathian Basin. In *Climate Change and Consequences* (in Hungarian) (ed.: *Dunkel, Z.*). *Meteorological Scientific Days '97*, November 20-21, 1997, Hungarian Meteorological Service, Budapest, 117-125.

Bartholy, J. and *Pongrácz, R.*, 1998: The differing trends of the Hungarian precipitation time series, areal and decadal changes of extreme precipitation (in Hungarian). In *Proc. of IIth Conference of Forest and Climate* (eds.: *Tar, K.* and *Szilágyi, K.*) Sopron, June 4-6, 1997, Kossuth University Press, Debrecen, 62-66.

Bárdossy, A. and *Plate, E.*, 1992: Space-time model for daily rainfall using atmospheric circulation patterns. *Water Resour. Res. 28*, 1247-1260.

Bárdossy, A., Duckstein, L. and *Bogárdi, I.*, 1995: Fuzzy rule-based classification of circulation patterns for precipitation events. *Int. J. Climatol. 15*, 1087-1097.

Boer, G.J., McFarlane, N.A. and *Laprise, R.*, 1984: The climatology of the Canadian Climate Centre General Circulation Model as obtained from a five-year simulation. *Atmos. Ocean 22*, 432-437.

Bogárdi, I., Matyasovszky, I., Bárdossy, A. and *Duckstein, L.*, 1993: Application of a space-time stochastic model for daily precipitation using atmospheric circulation patterns. *J. Geophys. Res. 98(D9)*, 16,653-16,667.

Böhm, R., 1992: Lufttemperaturschwankungen in Österreich seit 1775. *Österreichische Beiträge zu Meteorologie und Geophysik, Heft. 96.*

Brázdil, R., 1992: Reconstruction of the climate of Bohemia and Moravia in the last millennium – problems of data and methodology. *European climate reconstructed from documentary data: methods and results (*ed.: *Frenzel, B.)*, 75-86.

Breinman, L., Friedman, J.H., Olshen, A. and *Stone, J.C.*, 1984: *Classification and Regression Trees.* Wadsworth and Brooks, Monterey, Calif.

Cubash, U., Hasselmann, K.-Hock, H., Maier-Reimer, E.-Mikolajewicz and *U.-Santer, B.D.*, 1991: *Time-dependent greenhouse warming computations with a coupled ocean-atmosphere model.* Max Planck Inst. Meteorolol., 67.

Domonkos, P., 1998: Statistical characteristics of extreme temperature anomaly groups in Hungary. *Theor. Appl. Climatol. 59*, 165-180.

Faragó, T., Iványi, Zs. and *Szalai, S.* (eds.), 1990: Climate variability and change – I. Causes, processes, regional impacts with special emphasis on the socio-economic impacts and the tasks related to the international cooperation (in Hungarian). *Hungarian Ministry for Environment and Regional Policy, Hungarian Meteorological Service*, Budapest, 100 p.

Faragó, T., Iványi, Zs. and *Szalai, S.* (eds.), 1991: Climate variability and change – II. Changes in composition of atmosphere and in the climatic characteristics, detection, modelling, scenarios and impacts of the regional changes. Summary (in Hungarian). *Hungarian Ministry for Environment and Regional Policy, Hungarian Meteorological Service*, Budapest, 31 p.

Faragó, T. (ed.), 1998: Stabilisation of the greenhouse gas emissions: The Kyoto Protocol. Adoption of the Kyoto Protocol to the United Nations framework Convention on Climate Change and agenda in Hungary. *Hungarian Commission on Sustainable Development*, Budapest, 96 p.

Giorgi, F. and *Mearns, L.O.*, 1991: Approaches to the simulation of regional climate change: a review. *Reviews of Geophysics 29*, 191-216.

Giorgi, F., Marinucci, M.R. and *Visconti, G.*, 1992: A $2\times CO_2$ climate change scenario over Europe generated using a Limited Area Model nested in a General Circulation Model. II: Climate Change Scenario. *J. Geophys. Res. 97*, 10011-10028.

Giorgi, F., Mearns, L.O., Bogárdi, I., Matyasovszky, I. and *Palecki, M.*, 1999: Comparison of climate change scenarios generated from regional climate model experiments and empirical downscaling. Special issue on new developments and applications with the NCAR Regional Climate Model (RegCM). *J. Geophys. Res. 104(D6)*, 6603-6621.

Harnos, Zs., 1998: Expected climate tendencies and their impact on the production of some crops. In *Climate Change and Consequences* (in Hungarian) (ed.: *Dunkel, Z.*). *Meteorological Scientific Days'97*, November 20-21, 1997, Hungarian Meteorological Service, Budapest, 55-66.

Hess, P. and *Brezowsky, H.*, 1969: *Katalog der Groswetterlagen Europas.* Berichte des Deutchen Wetterdienstes Nr. 113, Bd. 15, 2. neu bearbeitete und erganzte Aufl., Offenbach a. Main, Selbstverlag des Deutschen Wetterdienstes.

Iványi, Zs., 1995: Variation of daily extreme temperatures in Hungary. *Időjárás 99*, 85-92.

Kertész, Á., Lóczy, D., Mika, J., Papp, S., Huszár, T. and *Sántha, A.*, 1999: Studies on the impact of global climate change on some environmental factors in Hungary. *Időjárás 103*, 37-65.

Koflanovits-Adámy, E. and *Szentimrey, T.*: 1986: The variations of the precipitation amounts in the Charpathian Basin during the present century (in Hungarian). *Időjárás 90*, 206-216.

Kovács, G. and *Dunkel, Z.*, 1998: : Assessment of the impacts of climate change on arable lands of Hungary for the next half century (in Hungarian). In *Climate Change and Consequences* (ed.:

Dunkel, Z.). *Meteorological Scientific Days '97*, November 20-21, 1997, Hungarian Meteorological Service, Budapest, 181-193.

Kovács-Láng, E., Kröel-Dulay, Gy., Kertész, M., Mika, J., Rédei, T., Rajkai, K., Hahn, I. and *Bartha, S.*, 1998: Change of the gap dynamics of succession in a semiarid gradient for the perennial open sandy steppe (in Hungarian). In *Climate Change and Consequences* (ed.: *Dunkel, Z.*). *Meteorological Scientific Days '97*, November 20-21, 1997, Hungarian Meteorological Service, Budapest, 43-54.

Marinucci, M.R., Giorgi, F., Beniston, M., Id, M., Chuck, P., Okamura, A. and *Bernasconi, A.*, 1995: High resolution simulations of January and July climate over the western alpine region with a nested regional modeling system. *Theor. Appl. Climatol. 51*, 119-138.

Matyasovszky, I., Bogárdi, I., Bárdossy, A. and *Duckstein, L.*, 1993: Space-time precipitation reflecting climate change. *Hydrol. Sci. J. 38*, 539-558.

Matyasovszky, I., Bogárdi, I., Bárdossy, A. and *Duckstein, L.*, 1994a: Local temperature estimation under climate change. *Theor. Appl. Climatol. 50*, 1-13.

Matyasovszky, I., Bogárdi, I. and *Duckstein, L.*, 1994b: Comparison of two general circulation models to downscale temperature and precipitation under climate change. *Water Resour. Res. 30*, 3437-3448.

Matyasovszky, I., Bogárdi, I. and *Ganoulis, J.*, 1995: Impact of global climate change on temperature and precipitation in Greece. *Appl. Math. Comp. 70*, 1-35.

Mátyás, Cs., 1997: Effects of environmental change on the productivity of tree populations. In *Perspectives of forest genetics and tree breeding in a changing world. IUFRO World Series* (ed.: *Mátyás, Cs.*), Vol. 6., Vienna, 109-121.

McGregor, J.L., 1997: Regional climate modelling. *Meteorol. Atmos. Phys. 63*, 105-117.

Mika, J., 1988: Regional features of global warming in Carpathian Basin (in Hungarian). *Időjárás 92*, 178-189.

Mika, J., 1991: Predictable impacts of a major global warming in Hungary (in Hungarian). *Időjárás 95*, 265-278.

Mika, J., 1992: Method of slices to estimate regional features of the global warming at extratropical latitudes. *Proc. of 5th Int. Meeting on Statistical Climatology*, June 22-26, 1992, Toronto, Canada , 433-436.

Mika, J., Ambrózy, P., Bartholy, J., Nemes, Cs. and *Pálvölgyi, T.*, 1995: Time variability of the climate of the Hungarian plains Alföld (in Hungarian). *Vízügyi Közlemények LXXVII*, 261-286.

Molnár, K., 1996a: Trend of precipitation amount in Hungary (in Hungarian). *Természet Világa*, Special Issue, 66-68.

Molnár, K., 1996b: Areal distribution of temperature and precipitation trends in Hungary for 110 years (1881-1990) (in Hungarian). *Földrajzi Értesítő XLV*, 23-33.

Molnár, K., 1996c: Temperature and precipitation trends for Hungary. *Proc. of 17th International Conference on Carpathian Meteorology*, October 14-18, 1996, Visegrád, Hungary, 161-166.

Molnár, K. and *Mika, J.*, 1997: Climate as a changing component of landscape: recent evidence and projections for Hungary. *Z. Geomorph. N.F.* Suppl.-Bd. 110, 185-195.

Muster, H., Bárdossy, A. and *Duckstein, L.*, 1994: Adaptive neuro-fuzzy modeling of a non-stationary hydrologic variable. *Proc. of International Symposium on Water Resources Planning in Changing World.* Karlsruhe, Germany, June 1994, II/221-230.

Nachtnebel, H.P., Hebenstreit, K., Bogárdi, I. and *Matyasovszky, I.*, 1996: Effect of climate change on the hydrology of an alpine watershed (in German). *Proc. of Internationales Symposium am 27-28. November 1995 im Europaischen Patentamt in München*, Institut für Wasserwesen, Heft 56b, 307-331.

Péczely, Gy., 1981: *Climatology* (in Hungarian). Tankönyvkiadó, Budapest, 336 p.

Práger, T. and *Kovács, E.*, 1988: Investigation of effects of atmospheric trace gaese and aerosol particles on climate with a radiative convective model (in Hugarian). *Időjárás 92*, 153-162.

Rácz, L., 1999: *Climate History of Hungary Since 16th Century: Past, Present and Future*. Centre for Regional Studies of Hungarian Academy of Sciences, Pécs, No. 28., 160 p.

Szentimrey, T., 1995: General problems of the estimation of inhomogeneities, optimal weighting of the reference stations. *Proc. of 6th International Meeting on Statistical Climatology.* 19-23 June 1995, Galway, Ireland, 62-63.

Szentimrey, T., 1996: Some statistical problems of homogenisation: break points detection, weighting of reference series. *Proc. of 13th Conference on Probability and Statistics in the Atmospheric Sciences.* 21-23 February 1996, San Francisco, California, 365-368.

Tar, K., 1992: Climate of Túrkeve (in Hungarian). *Proc. of Conference on 145 Anniversary of the Birth of Hegyfoky Kabos*. Debrecen, Túrkeve, 156-164.

Tóth, Z., and Szentimrey, T., 1990: The binormal distribution: A distribution for representing asymmetrical but normal-like weather elements. *J. Climate 3*, 128-136.

Weidinger, T., Matyasovszky, I. and *Bogárdi, I.*, 1994: The influence of atmospheric circulation on the water budget of Lake Balaton. *Meteorol. Zeitschrift, N.F. 3*, 288-296.

Weidinger, T., Matyasovszky, I., Bartholy, J. and *Bogárdi, I.*, 1995: Climate change impact on daily pan evaporation. *Meteorol. Zeitschrift, N.F. 4* , 235-245.

Wilson, L.L., Lettenmaier, D.P. and *Skyllingstad, E.*, 1992: A hierarchical stochastic model of large scale atmospheric circulation patterns and multiple station daily precipitation. *J. Geoph. Res. 97*, 2791-2809.

IDŐJÁRÁS

Quarterly Journal of the Hungarian Meteorological Service
Vol. 105, No. 1, January–March 2001, pp. 19–28

Investigation of surface-atmosphere heat exchange processes using surface and satellite measurements

Judit Kerényi[1] and **Iván Csiszár**[2]

[1]*Hungarian Meteorological Service, Satellite Research Laboratory,*
P.O. Box 39, 1675-Budapest, Hungary; E-mail: kerenyi.j@met.hu

[2]*Cooperative Institute for Research in the Atmosphere*
National Oceanic and Atmospheric Administration
National Environmental Satellite Data and Information Service
Office of Research and Applications
Camp Springs, MD, U.S.A.; E-mail: ivan.csiszar@noaa.gov

(Manuscript received 20 February 2001; in final form 27 February 2001)

Abstract—Seasonal changes in surface-atmosphere heat exchange processes were studied over diverse vegetated surfaces by the synergy of ground observations and satellite measurements over two target areas in Hungary. NOAA Advanced Very High Resolution Radiometer (AVHRR) Global Area Coverage (GAC) data and the NOAA Global Vegetation Index (GVI) weekly data set were combined with conventional ground observations from meteorological stations. Multi-year mean seasonal cycles of satellite-derived parameters were derived and compared. The temporal variation of day- and nighttime temperature difference (DNTD) proved to be directly related to that of latent heat exchange through vegetation conditions and precipitation. Sensible heat flux was characterized by the air-skin temperature difference. The observed differences over the two target areas can be attributed to differences in the dominant vegetation. Time series of DNTD, derived from daytime GVI temperature data and nighttime minimum soil temperature, exhibited significant interannual variability also.

1. Introduction

The derivation of large-scale continuous fields of surface characteristics is possible only by the use of high-or moderate spatial resolution satellite imager data. The Advanced Very High (spectral) Resolution Radiometer (AVHRR) on board the operational polar orbiting NOAA satellites provides top-of-the atmosphere measurements in five atmospheric window channels in the visible to infrared range of the radiometric spectrum. The current configuration of NOAA's Polar Orbiting Environmental Satellite System (POES), consisting of one "morning"

and one "afternoon" operational satellite, allows four views of a given target area for most of the globe. The multispectral information from AVHRR can be analysed to derive a number of surface and atmospheric parameters, many of which were not planned to be studied by this instrument during it's design.

Many of the AVHRR-derived parameters can be used to describe the thermo-physical properties of land surface and to characterize the surface energy exchange processes. The surface energy balance can be described by the following equation (see, for example, *Dunkel et al.*, 1991):

$$R_n = G + H + LE \tag{1}$$

where R_n is the net radiation flux, G is the soil heat flux, H is the (vertical) sensible heat flux and LE is the (vertical) latent heat flux. There have been numerous theoretical and empirical studies to quantify these parameters from satellite data and to produce high-resolution maps of them (*Seguin* and *Itier*, 1983; *Hurtado et al.*, 1994; *Choudhury*, 1994; *Tarpley*, 1994; *Diak et al.*, 1995; etc.). In this paper we rather focus on describing the temporal variation of satellite-derived surface parameters that are related to the above fluxes. It is thus not our goal to derive accurate quantitative estimates of all fluxes, but rather to compare the interrelation of their temporal changes over the growing season.

A combination of the visible (*VIS*) and near-IR (*NIR*) measurements of AVHRR, the Normalized Difference Vegetation Index, $NDVI = (NIR - VIS)/(NIR + VIS)$ provides information on the amount and state of vegetation cover. This parameter can be further used to derive higher-level products, such as the fraction of green vegetation or leaf area index (*Price*, 1993; *Nemani et al.*, 1996; *Gutman* and *Ignatov*, 1998; *Carlson* and *Ripley*, 1999). NDVI is also an important parameter in land cover classification schemes *(DeFries* and *Townshend*, 1994).

Surface temperature measurements from AVHRR, taken at different local times can be used for the reconstruction of the diurnal temperature cycle, and it's amplitude, the diurnal temperature range (DTR), which latter is an important surface characteristic related to thermal inertia (*Price*, 1985; *Tänczer et al.*, 1995; *Sobrino* and *Kharraz*, 1999). DTR is a good indicator of surface moisture conditions through evaporation from bare soil and evapotranspiration by vegetation, and also the long-term monitoring of land cover change from desertification, de- or reforestation, wildfires etc.

A combination of satellite-derived parameters with conventional measurements at the ground provides further opportunity for the characterization of energy fluxes near the surface. Here we used the difference between the surface skin temperature and the maximum air temperature to characterize the daily maximum sensible heat flux at the surface. In the analysis ground measurements of precipitation were also used as a control parameter to characterize surface moisture conditions. The seasonal changes of surface conditions were studied over two target areas in Hungary with different vegetation cover.

The results of such a study are sensitive to any inaccuracies of the input data and to artifacts inherent in the observational system. The orbital drift of the "afternoon" NOAA satellites introduces spurious interannual trends in observed surface reflectances (and NDVI to a smaller extent) because of the bidirectional effects due to changing solar illumination angle and also in surface temperatures, mostly because of the changing local time of observation. Imperfections in preprocessing, such as calibration and cloud screening, may introduce additional errors. Therefore a careful analysis and processing of the original satellite data is required before the detailed physical analysis.

In the remaining of this paper, Section 2 of this paper presents the data used for our analysis. The methodology and the results are discussed in Sections 3 and 4 respectively, followed by the conclusions in Section 5.

2. Data

2.1 Surface data

The surface data used in this study were measured at the meteorological stations at Szarvas (46.52°N, 20.34°E) and Keszthely (46.46°N, 17.15°E). They include daily maximum and minimum air temperatures at 2 m (T_{max}, T_{min}), the daily minimum near-ground temperature (*Radmin*, measured at 2 cm and often referred to as *radiative minimum temperature*), and daily precipitation amount. Szarvas is located in a mostly agricultural area, whereas the area around Keszthely is a mixture of forests, marshlands and croplands. The climate in Keszthely is more affected by oceanic influence, resulting in somewhat higher annual precipitation amount and smaller annual temperature variability.

2.2 Satellite data

Global Area Coverage (GAC) 4-km data are produced by sampling and averaging onboard satellite from the full 1-km resolution AVHRR measurements in five wavebands: the visible (VIS, 0.58–0.68 μm, channel 1), near-IR (NIR, 0.73–1.1 μm, channel 2), mid-infrared (3.6–3.9 μm, channel 3) and thermal infrared (IR, 10.3–11.3 and 11.5–12.5 μm, channels 4 and 5, respectively). Daytime and nighttime GAC data have been archived at NOAA/NESDIS for the two target areas since July 1993.

From the GAC raw data visible and near-IR reflectances were derived using the time-dependent post-launch calibration coefficients (*Rao* and *Chen*, 1995, 1996). The reflectances were combined into NDVI. Channel 4 and 5 brightness temperatures, T_4 and T_5, were derived from observed radiances using on-board calibration coefficients. Channel 3 reflectance (used to detect snow contamination in early spring) was calculated following the approach by *Stowe et al.* (1999) in removing the thermal component based on T_4 and T_5. Data from this dataset will hereafter referred to as GAC Target Dataset (GTD) data.

The operational NOAA Global Vegetation Index (GVI) weekly dataset (*Kidwell*, 1997) is produced from afternoon GAC observations. It is sampled first in space (one pixel out of about 16 GAC pixels on a daily basis within each gridbox of a 0.15° by 0.15° resolution Plate Carree grid) and then in time (one observation per week from the sampled daily data). The temporal compositing is done by taking observations corresponding to the maximum NIR- and VIS count difference over the seven-day period within each gridbox, ensuring the selection of the data that are least affected by clouds and aerosol. The calibration of the visible, NIR and IR data was done similarly to the GTD data. Both GTD and GVI data were screened for cloud contamination. Daytime GTD data were screened by the spatial heterogeneity technique of *Coakley* and *Bretherton* (1982) applied to visible reflectances. Residual clouds were screened out by $T_4 - T_{max}$ and visible reflectance threshold tests. Finally, outliers in visible reflectance in each 10-degree bin of satellite zenith angle were eliminated. Nighttime GTD data were screened by the Coakley and Bretherton method applied to T_4 and by a $T_4 - T_{min}$ threshold test. GVI data were screened for residual clouds by examining the departure of the weekly T_4 value from multi-year means (*Gutman et al.*, 1995).

3. Method

For compatibility between satellite observations from different years, we performed corrections for post-launch calibration errors and satellite orbital drift effects in VIS, NIR and NDVI using the parameterization by *Gutman* (1999a), which normalizes the observed reflectances to a common solar zenith angle. Similarly, brightness temperature data were also normalized to a common local observation time by the formulae of *Gutman* (1999b). NOAA-11 AVHRR data from July 1993–December 1994 were not used in this regional study because of the increasing uncertainty in the accuracy of these correction schemes for extreme observational conditions caused by the large satellite orbital drift towards the end of the satellites' lifetime.

The corrected T_4 and T_5 values in both AVHRR datasets were combined into Land Surface Temperature (T_s) using a split-window equation (*Gutman*, 1994) including the emissivity (ε) correction based on *NDVI* (*Van de Griend* and *Owe*, 1993):

$$T_s = T_4 + 2.63 \times (T_4 - T_5) + 1.274 + (T_4 + T_5)/2 \times (0.156 + 3.98 \times (T_4 - T_5)/(T_4 + T_5)) \times (1 - \varepsilon)/\varepsilon, \quad (2)$$

where $\varepsilon = 1.013 + 0.0681 \times \ln(NDVI)$.

The satellite-derived parameters were derived and averaged over 50×50 km rectangular areas around the meteorological stations in Szarvas and Keszthely.

It has been shown that the daytime and nighttime observations from the AVHRR sensor are good indicators of the diurnal temperature range (*Csiszár* and *Kerényi*, 1995) and thus the massive processing of 3-hour geostationary METEOSAT data is not necessary to characterize daily temperature variations. Note, however, that as the afternoon AVHRR observations deviate to some extent from the daily maximum temperatures, absolute values of DTR cannot be readily derived from AVHRR observations. In this paper we will use the AVHRR day-night difference (DNTD) values, which are smaller than, but well correlated with the maximum temperature range. The 10-day DNTD was derived from the cloud free daytime ($T_s(d)$) and nighttime ($T_s(n)$) surface temperature values from AVHRR only. As the daytime and nighttime GTD data were very rarely cloud free on the same day, maximum value compositing was not possible. Therefore 10-day mean DNTD was calculated from the 10-day mean $T_s(d)$ and the 10-day mean $T_s(n)$ values. Consequently, 10-day mean NDVI and the $(T_s(d)) - (T_{max})$ differences were calculated from the GTD data.

In the case of the GVI dataset, which includes only daytime observations, $T_s(n)$ was substituted by Radmin to derive DNTD. To check the applicability of this parameter we compared the Radmin values with the $T_s(n)$ values derived from GTD data for two years when both data were available. *Fig. 1* shows that the difference between the two kinds of data is within 2–3 degrees. It is also obvious that $T_s(d)$ tends to be more variable in time than $T_s(n)$ and thus DNTD is mostly driven by changes of $T_s(d)$.

4. Results

The annual variation of NDVI, DNTD and the $T_s(d) - T_{max}$ difference was derived using GTD data for the 1996–1998 period. *Fig. 2* shows the 3-year mean values of these parameters at Szarvas and Keszthely targets. Comparing the NDVI values at the two targets one can see an earlier greenup in spring at the Szarvas target with maximum NDVI in June, whereas at the Keszthely target the greenup started later, but NDVI decreased only in September. We can also see that in both targets DNTD increases at the beginning of the year. At the end of May, when vegetation has reached a certain stage of development with the corresponding evepotranspiration—NDVI is about 0.3—the DNTD increase quickly reverses, and after a few weeks it levels off at a lower value. In Szarvas, however, there is a weaker secondary maximum at the end of summer, which can be explained by the fact that solar irradiation is still high, but the vegetation cover is low.

The $T_s(d) - T_{max}$ difference closely follows the variation of DNTD. This suggests that the daytime-only GVI temperature data still hold useful information about surface heat exchange processes, which should be further examined in the future.

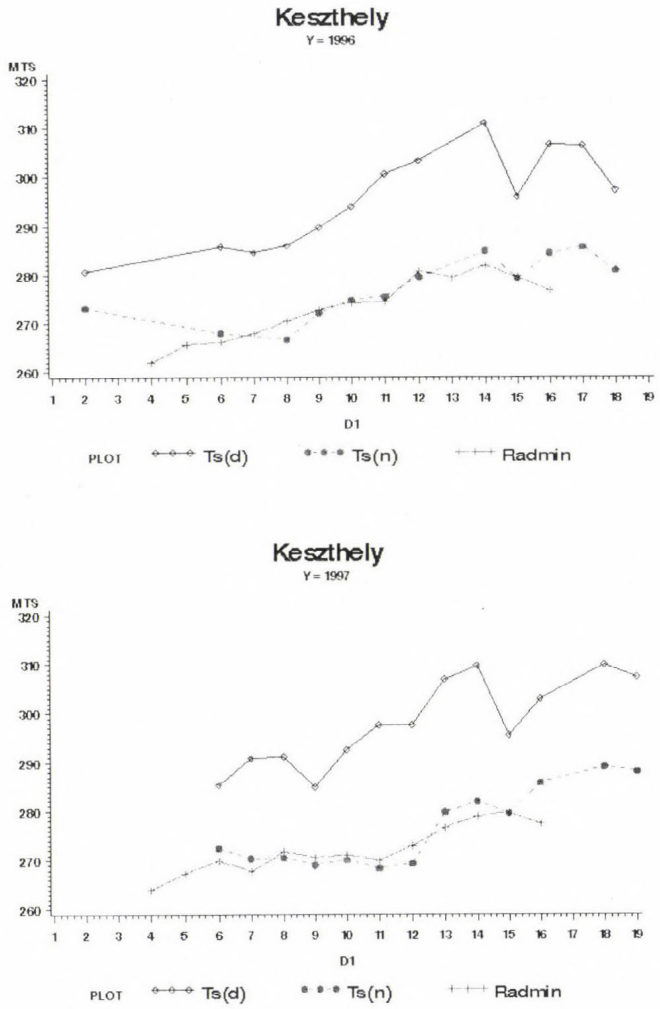

Fig. 1. Daytime ($T_s(d)$) and nighttime ($T_s(n)$) surface temperature [K] derived from GTD data and the radiation minimum temperature at the Keszthely target in 1996 and 1997. The horizontal axis denotes dekades of Julian days.

Figs. 3 and *4* show examples of temporal variation of NDVI, DNTD and precipitation in individual years over the Szarvas and Keszthely target areas respectively. Here the AVHRR data were taken from the GVI dataset for compatibility between years over a longer period. One can clearly see that DNTD is directly related to evaporation, i.e. the combined effect of soil moisture and vegetation condition. Also, to analyze DNTD in a certain months, history from the previous several months needs to be considered. In 1992 in Szarvas, the greenup started quite early, despite the low precipitation amount (probably temperature

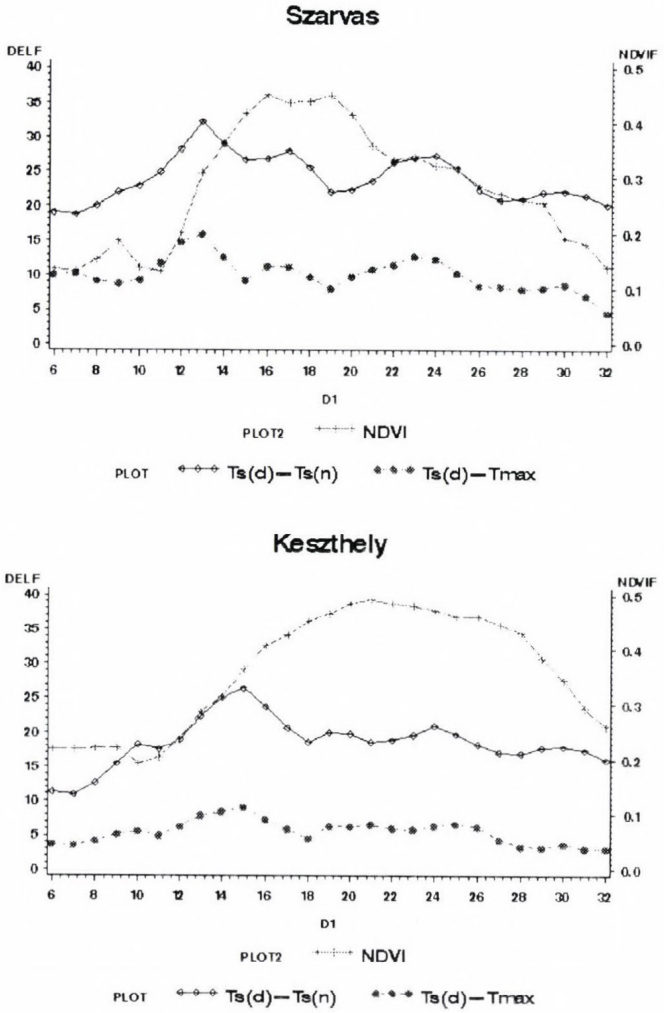

Fig. 2. The annual variation of the 3-year mean value of *NDVI*, $T_s(d) - T_s(n)$ (= *DNTD*) and $T_s(d) - T_{max}$ [K] at Szarvas and Keszthely. The horizontal axis denotes dekades of Julian days.

conditions were still favorable). However, because the soil moisture content was low, DNTD was still high until May. It decreased only in June, with increased rainfall, although the vegetation conditions were not so good because of the prolonged dry period earlier. In 1998 in Szarvas, precipitation was high in spring, but there was a delay in vegetation development, and thus evapotranspiration could not suppress the DNTD values. DNTD decreased again in June, this time because by then vegetation growth had reached the stage when evapotranspiration could efficiently use the abundant soil moisture from the previous months.

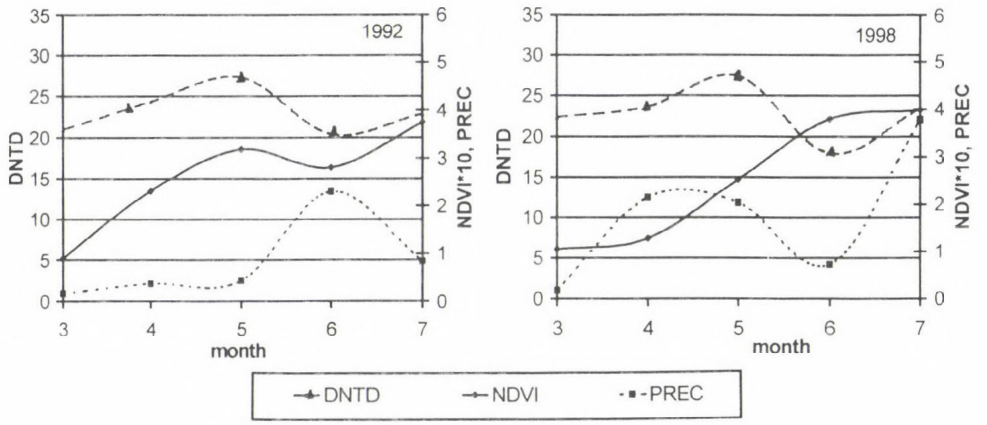

Fig. 3. The annual variation of NDVI, precipitation [mm] and DNTD [K] at Szarvas station in 1992 and 1998.

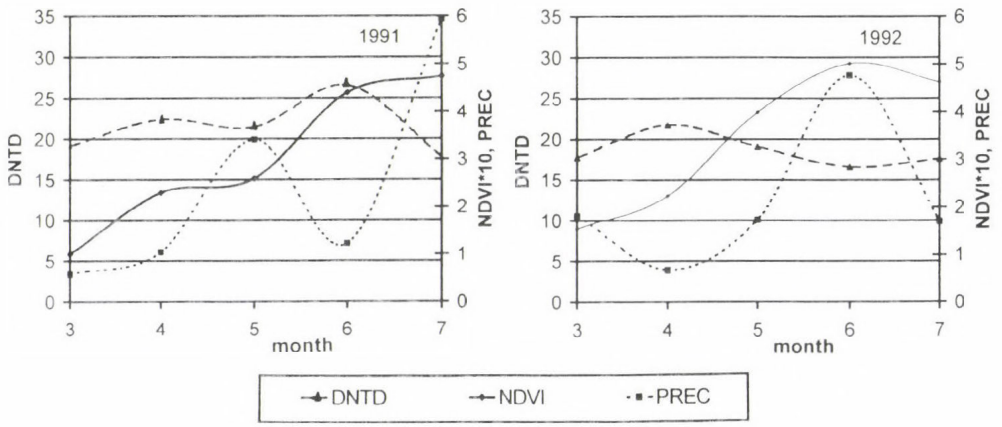

Fig. 4. The annual variation of NDVI, precipitation [mm] and DNTD [K] at Keszthely station in 1991 and 1992.

In Keszthely precipitation amount was relatively high in May 1991. It immediately shows in the temporary small decrease of DNTD. In June, with high NDVI and low precipitation, DNTD still remains high, probably much of the moisture from the May precipitation was efficiently removed from the soil in May. In 1998, the low DNTD values in May and June are the obvious results of high precipitation amount and well developed vegetation.

5. Conclusions

Results from our study have served as examples of the combination of satellite and surface data to efficiently study intra- and inter-annual changes in surface-atmosphere heat exchange processes. DNTD is a good indicator of latent heat exchange through direct evaporation from soil and evapotranspiration from vegetation. As such, it is also indirectly related to soil moisture, precipitation and vegetation condition. Both DNTD and the air-skin temperature difference (an indicator of sensible heat flux) are mostly driven by daytime temperature.

Time series of the various parameters also have shown that the surface processes can be understood only by the synergistic analysis of the different components of the surface—atmosphere system. On the other hand, the signature in the satellite-derived quantities, particularly NDVI and DNTD, is an integrated result of various current processes as well as their time history during the previous period. Analysis of separate spectral reflectances (*Gutman et al.*, 2000) or separate daytime and nighttime temperatures can thus reveal further details of the processes. For example, analysis of absolute temperature values and their anomalies is helpful in explaining vegetation conditions (*Kogan*, 1997).

Acknowledgement—This work has been supported by the US-Hungarian Science and Technology Joint Fund (No. 548) and the Hungarian Scientific Research Funds (No. T25543).

References

Carlson, T.N. and *Ripley, D.N.*, 1999: On the relation between NDVI, fractional vegetation cover and leaf area index. *Remote Sens. Environ 62*, 241-252.

Choudhury, J.B., 1994: Synergism of multispectral satellite observations for estimating regional land surface evaporation. *Remote Sens. Environ. 49*, 264-274.

Coakley, J.A. and *Bretherton, F.P.*, 1982: Cloud cover from high-resolution scanner data: Detecting and allowing for partially filled fields of view. *J. Geophys. Res. 87*, 4917-4932.

Csiszár, I. and *J.Kerényi*, J., 1995: The effect of the vegetation index on the daily variation of the active surface temperature. *Adv. Space Res. 16.*, No.10, (10)177–(10)180.

DeFries, R. and *Townshend, J.R.G.*, 1994: NDVI-derived land cover classification at global scales. *Int. J. Remote Sens. 15*, 3567-3586.

Diak, G. R., Rabin, R.M., Gallo, K. and *Neale, C.M.*, 1995: Regional-scale comparisons of vegetation and soil wetness with surface energy budget properties from satellite and in-situ observations. *Remote Sensing Reviews 12*, 355-382.

Dunkel, Z., Pásztor, K. and *Tiringer, C.*, 1991: Calculation of diurnal variation of surface temperature using a simplified energy balance model. *Időjárás 95*, 170-177.

Van de Griend, A.A. and *Owe, M.*, 1993: On the relationship between thermal emissivity and the normalized difference vegetation index for natural surfaces. *Int. J. Remote Sens. 14*, 1119-1131.

Gutman, G., 1994: Multi-annual time series of AVHRR-derived land surface temperature. *Adv. Space Res. 14*, (3)27-(3)30.

Gutman, G., Csiszár, I. and *Romanov, P.*, 2000: Using NOAA/AVHRR products to monitor El Niño impacts: Focus on Indonesia in 1997–1998. *Bull. Amer. Meteorol. Soc. 81*, 1189-1205.

Gutman, G., Tarpley, D., Ignatov, A. and *Olson, S.*, 1995: The enhanced NOAA Global Land Dataset from the Advanced Very High Resolution Radiometer. *Bull. Amer. Meteorol. Soc. 76*, 1141-1156.

Gutman G. and *Ignatov, A.*, 1998: The derivation of the green vegetation fraction from NOAA/AVHRR data for use in numerical weather prediction models. *Int. J. Rem. Sens. 19*, 1533-1543.

Gutman, G., 1999a: On the use of long-term global data of land reflectances and vegetation indices derived from the advanced very high resolution radiometer. *J. Geophys. Res. 104*, D6, 6241-6255.

Gutman, G., 1999b: On the monitoring of land surface temperatures with the NOAA/AVHRR: Removing the effect of satellite orbit drift. *Int. J. Remote Sens. 20*, 3407-3413.

Hurtado, E., Artigao, M.M. and *Caselles, V.*, 1994: Estimating maize (Zea mays) evapotranspiration from NOAA-AVHRR thermal data in the Albacete area, Spain. *Int. J Remote Sensing* **15**, 2023-2037.

Ignatov, A. and *Gutman, G.*, 1999: Monthly mean diurnal cycles in surface temperatures over land for global climate studies. *J. Climate 12*, 1900-1910.

Jin, M. and *Dickinson, R.E.*, 1999: Interpolation of surface radiative temperature measured from polar orbiting satellites to diurnal cycle. *J. Gephys. Res. 104*, 2105-2116.

Kidwell, K, 1997: *Global Vegetation Users' Guide*. NOAA/NESDIS National Climatic Data Center, U.S Dep. of Commer., Washington, D.C.

Kogan, F.N., 1997: Global drought watch from space. *Bulletin Amer. Meteorol. Soc. 78*, 621-636.

Nemani, R.R., Running, S.W., Pielke, R.A. and *Chase, T.N.*, 1996: Global vegetation cover changes from coarse resolution satellite data. *J. Geophys. Res. 101*, 7157-7162.

Price, J.C., 1985: On the analysis of thermal infrared imagery: The limited utility of apparent thermal inertia. *Remote Sens. Environ. 18*, 59-73.

Price, J.C., 1993: Estimating leaf area index from satellite data. *IEEE Transactions Geosci. Remote Sens. 31*, 727-734.

Rao, C.R.N. and *Chen, J.*, 1995: Intersatellite calibration linkages for the visible and near-infrared channels of the advanced very high resolution radiometer on the NOAA 7, 9, 11 spacecraft. *Int. J. Remote Sens. 16*, 1931-1942.

Rao, C.R.N. and *Chen, J.*, 1996: Postlaunch calibration of the visible and near-infrared channels of the advanced very high resolution radiometer on the NOAA 14 spacecraft, 1. *Int. J. Remote Sens. 17*, 2743-2747.

Seguin, B. and *Itier, B.*, 1983: Using midday surface temperature to estimate daily evaporation from satellite thermal IR data. *Int. J. Remote Sensing 4*, 371-383.

Sobrino, J.A. and *El Kharraz, M.H.*, 1999: Combining afternoon and morning NOAA satellites for thermal inertia estimation 1. Algorithm and its testing with Hydrologic Atmospherci Pilot Experiment-Sahel data. *J Geophys. Res. 104*, 9445-9453.

Stowe, L., Davis, P. and *McClain, E.P.*, 1999: Scientific basis and initial evaluation of the CLAVR-1 global clear/cloud classification algorithm from the Advanced Very High Resolution Radiometer. *J. Atmos. Oceanic Technol. 16*, 656-681.

Tänczer, T., Rimóczi-Paál, A. and *Csiszár, I.*, 1995: Prediction of daily amplitudes of canopy temperatures using satellite information. *Adv. Space Res.* 16, (10)181-(10)184.

Tarpley, J.D., 1994: Monthly evapotranspiration from satellite and conventional meteorological observations. *J. Climate 7*, 704-713.

IDŐJÁRÁS

Quarterly Journal of the Hungarian Meteorological Service
Vol. 105, No. 1, January–March 2001, pp. 29–38

Visibility and fog forecasting based on decision tree method

Ferenc Wantuch

Hungarian Meteorological Service,
P.O. Box 38, H-1525 Budapest, Hungary; E-mail: wantuch.f@met.hu

(Manuscript received 6 April 2000; in final form 15 December 2000)

Abstract—The paper describes a visibility and fog forecasting model developed and used at the Hungarian Meteorological Service (HMS) for last 3 years. The investigated model is a perfect prognostical model (PP). Characteristics of the model, such as input data, statistical approach, decision trees and threshold numbers are described in this paper. The model was tested for both measured sounding and predicted data. Verification of the model led to very good results, so it was applied to aeronautical forecasting as well as to nowcasting. Information and short review about different types of other visibility models are also given.

Key-words: NWP parameters, perfect prognosis (PP), model output statistics (MOS), FOGSI index, decision tree.

1. Introduction

Visibility forecast is very important for transportation, especially for air traffic where its accuracy is prominent. The WMO/ICAO requirements are very rigorous in aviation meteorology (*ICAO*, 1998). Verifications of aeronautical forecasts show that the reason of poor terminal weather forecasts—in about 70 per cent of all cases—is a weak or not suitable visibility prediction. It have not been available any special numerical methods at the HMS before, which could be an aid for forecasters in the prediction of the visibility, so they could use only traditional tools.

The European forecasters use different methods in the practice. One possibility is the diagnosis of fog from satellite images (*Kerényi et al.*, 1995). Some organisations, e.g., EUMETSAT, Central Institute for Meteorology and Geodynamics Austria (ZAMG), Swedish Meteorological Institute (SMHI) and Météo France use NOAA AVHRR and Meteosat images in order to analyse fog

and low cloud from satellite data. Another possibility is the improvement of 1-D-models applied in UK, Sweden, Portugal, Belgium (*Stessel* and *Ottoy,* 1999) and also in France. Some case studies have been validated with promising results.

The third way is the use of statistical methods and decision support systems for fog and low cloud forecasting. In the frame of it different methods, like decision trees, linear regression, Kalman-filter (*Kilpinen,* 1992) and neural network (*Pasini et al.,* 1999) were considered for probability forecasts. In general, the results of all these methods were promising, so we considered the problem from statistical point of view.

Let us denote by y the estimated parameter, that is the predictand and by $x_1, x_2, ..., x_p$ the detected meteorological elements, which are the predictors. In this case we have to construct a function:

$$y = f(x_1, x_2, ..., x_p) + \varepsilon, \tag{1}$$

where ε is the error of the method. One can use this function in the following estimated form:

$$\tilde{y} = f(\tilde{x}_1, \tilde{x}_2, ..., \tilde{x}_p), \tag{2}$$

where $\tilde{x}_1, \tilde{x}_2, ..., \tilde{x}_p$ are known from NWP. This is the basic concept of the perfect prognosis method. Suppose that Eq. (2) is constructed directly from $\tilde{x}_1, \tilde{x}_2, ..., \tilde{x}_p$, so

$$y = f(\tilde{x}_1, \tilde{x}_2, ...\tilde{x}_{,p}) + \varepsilon. \tag{3}$$

In this way we get a model output statistical method. Based on this idea, an automatic visibility forecast method can be constructed. The input data of the visibility prediction is, in the given case, the ALADIN mesoscale model output. This is a hydrostatic, spectral limited area numerical weather prediction model, which was developed by collaboration among Météo-France and some Central- and East-European hydrometeorological services including HMS. The main dynamical characteristics of the model, like the preparation of initial and lateral boundary conditions, the physics and post-processing were discussed by *Horányi et al.* (1996).

In order to find a connection with visibility, first we made a comprehensive statistical research on direct measurements and derived physical quantities. The best correlation was received by the fog stability index. The index was calculated according to the following formula:

$$FOGSI = 2 \mid T_{sfc} - T_{850} \mid + 2\,(T_{sfc} - T_{d\,sfc}) + 2\,W_{850}, \tag{4}$$

where

T_{sfc} temperature near the surface,
$T_{d\,sfc}$ dew point near the surface,
T_{850} temperature on 850 hPa level,
W_{850} wind speed on 850 hPa level.

FOGSI index takes into account the temperature gradient (that is the measure of the stability), the impact of moisture near the surface and the mixing by wind.

2. Results of statistical research

The FOGSI index is highly correlated with the observed visibility, especially in autumn-winter time when fog and mist frequently occur. Because of the strong relationship, we could use a regression connection based on a two years long dataset as follows:

$$Visibility = -1.33 + 0.45 \times FOGSI \tag{5}$$

Fig. 1 shows connection between the FOGSI index and the observed visibility (measured in kms) in October 1996. Based on this figure we can make the following considerations. There is a critical interval of FOGSI. Above the upper limit of this interval the calculation of visibility by regression is adequate to use. On the other hand, if the FOGSI number is smaller than the lower limit of this domain, one can predict fog in all cases. The variance of the visibility values inside the critical interval is very high, consequently the statistical method is uncertain. It means that in this interval one can not decide about the visibility based on FOGSI, e.g., if FOGSI is equal to 25, it might represent fog, mist or good visibility at the same time. If data are taken into account only from the critical interval, then the statistical connection between FOGSI and visibility becomes very poor (*Fig. 2*). Its physical reason is that several other effects, which play a great role in development of visibility, were neglected in FOGSI definition. Therefore, one has to introduce some new weather predictors and methods. Parameters, which can be computed from TEMP data and NWP model output as well, are reasonable to select. After thorough investigation, the mean relative humidity of lower air layers (925 hPa - surface) and upper layers (850–700 hPa), the near surface wind speed and relative humidity were chosen to be included into the decision process.

Having examined a large number of cases, it was found that in winter period the cold air can be accumulated near the surface, mainly in the valleys and basins. Sometimes the surface temperature is 2–5 degrees colder than the temperature of the 850 hPa level, in extreme cases this difference reaches 10°C. This inversion stratification is called "the cold air pad" (*Tóth,*1984; *Bóna,*

1986), which represents a very stable state of the atmosphere. We came to the conclusion, that it is necessary to treat cold air pad situations separately and for these days other threshold numbers have to be determined. In order to specify different visibility categories inside the critical interval, one had to work out a new procedure. The steps of the process are summarized in *Fig. 3.*

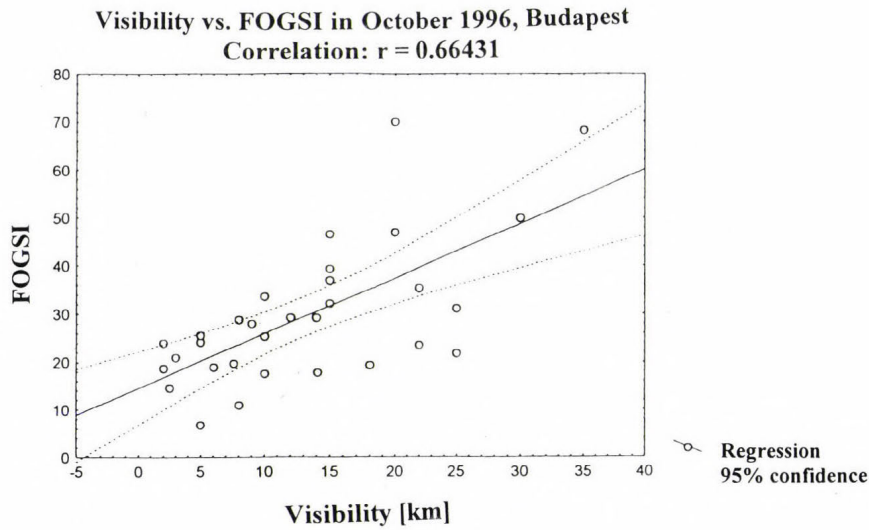

Fig. 1. Correlation between FOGSI and observed visibility.

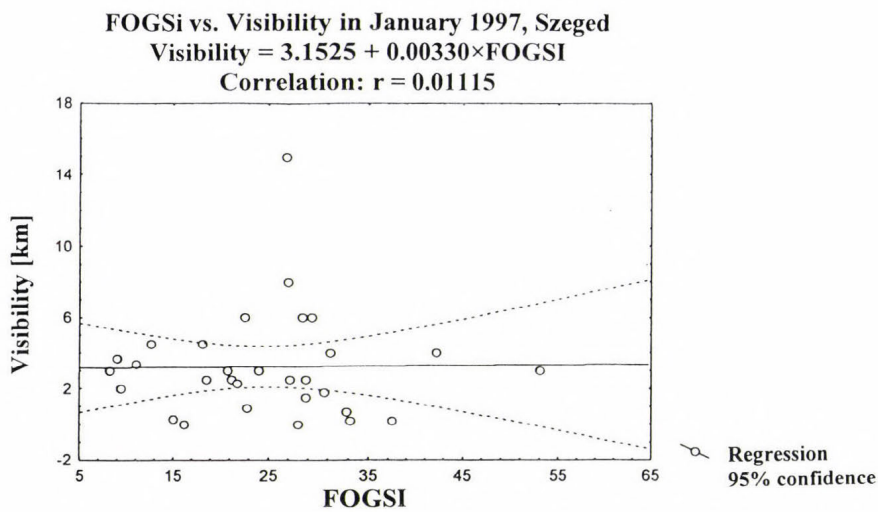

Fig. 2. Correlation between FOGSI and observed visibility (all data derived from critical domain).

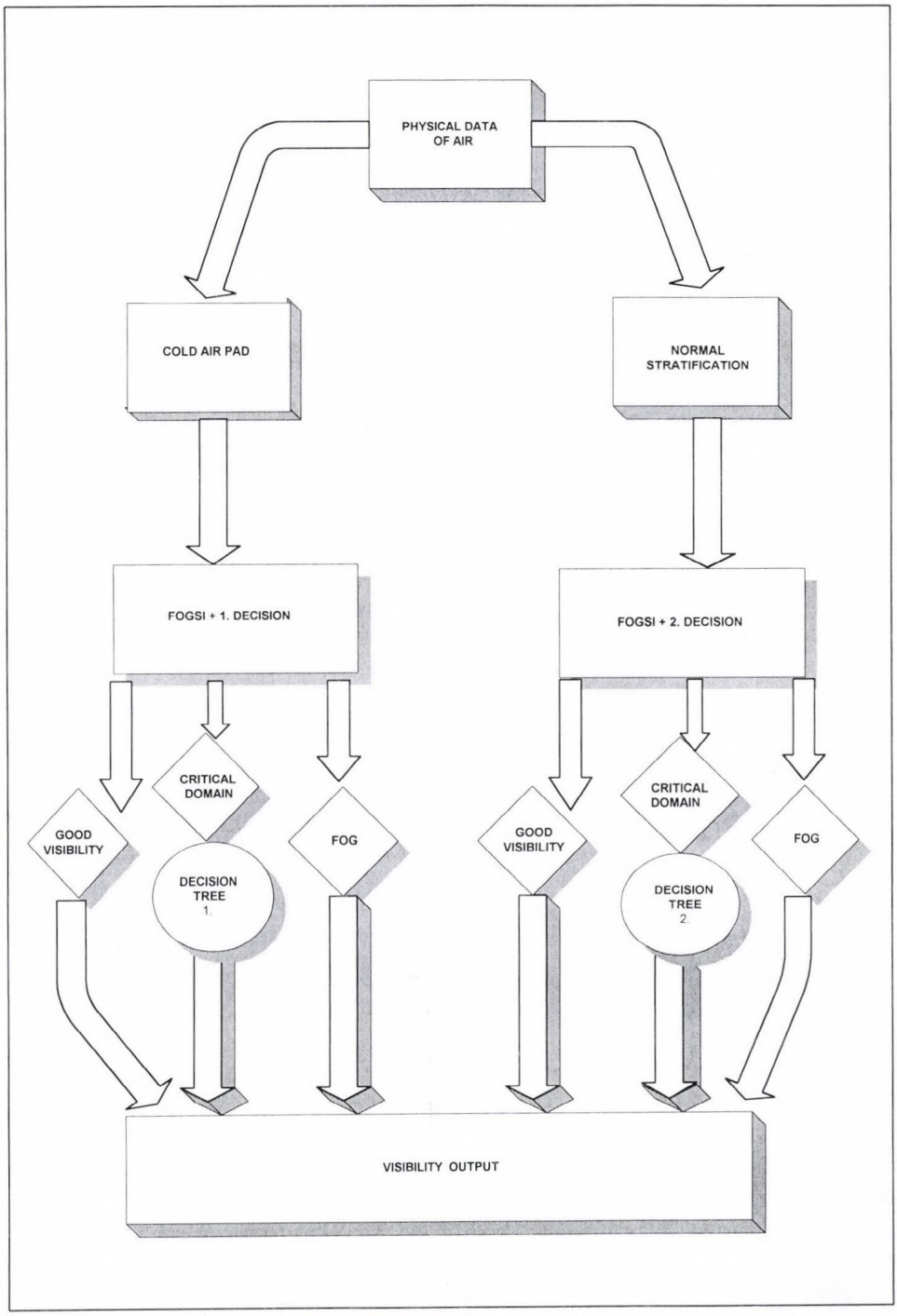

Fig. 3. The first steps of the process.

3. Decision tree

In this chapter the principles and steps of the decision-making procedure will be discussed and demonstrated in *Fig. 4*. Each box represents an important physical condition of the air column. The threshold numbers are based on two years of surface and radiosonde measurements of Budapest-Lőrinc.

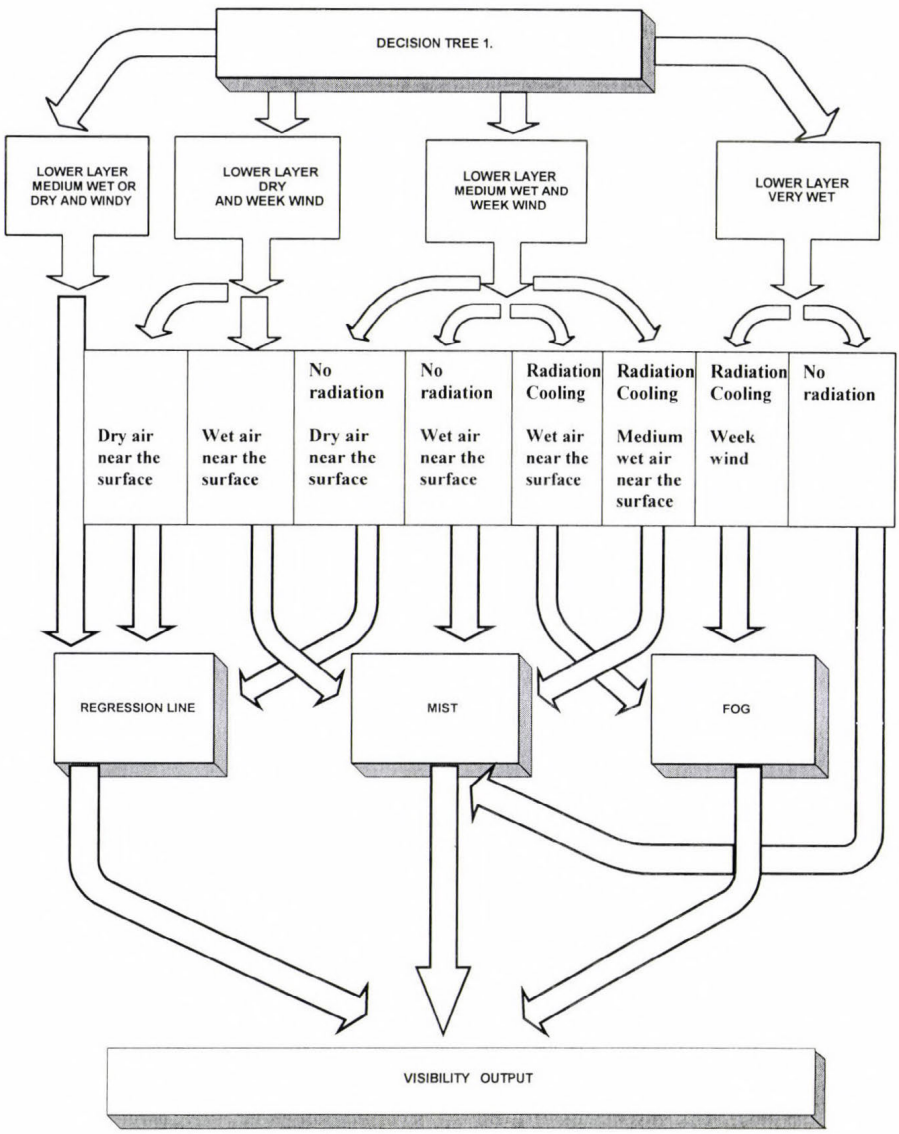

Fig. 4. Decision tree in case of normal stratification.

Suppose that the lowest layer of the air (between surface and 925 hPa) is dry or moderately wet and windy, then the visibility depends on the water content near the surface. In this case the process uses simply the regression line for determining the visibility. If the lowest layer is dry (relative humidity <80%) and the wind is weak, then the visibility depends on the water content of the air near the surface. If this layer is wet, then we choose mist, otherwise a good visibility category is selected. If the lowest layer is medium wet (80%< relative humidity <90%), then four subclasses are constructed. In these subclasses the radiative cooling effects of the atmosphere above a ground level point are represented. This influence is modeled as the difference of mean relative humidity between the upper and the lower layers as follows:

(1) If the air near the surface is dry and we do not include radiative cooling effect near the surface, then visibility can be calculated by the help of the regression line.
(2) If the air near the surface is wet and we have no radiative cooling influence in the air column, then the decision is the misty weather.
(3) If the air near the ground level is wet and we have radiative cooling effect, then fog formation is expected.
(4) If the air near the surface is medium wet and we include radiative cooling, misty weather is predicted.
(5) Finally, supposing that the air near the ground level is very wet (relative humidity >90%), then in case of radiative cooling we expect foggy, otherwise misty category.

For cold air pad situations similar decision tree was constructed. The main differences are in the values of the threshold numbers. If very high relative humidity and weak winds occur together, it will be foggy weather.

4. Test results

The test of diagnostic method presented in this paper led to the following results. *Fig. 5* illustrates the visibility at 00 UTC for each day of January in 1997, where JANAKTL means the measured, JANMODSZ the computed values. With regard to reliable visibility forecast, good estimation of the small values is especially important. As it is shown, under 5 km both lines give similar range of sight, even if the dotted line sometimes a little bit underestimates the real data, so it makes the prediction more safe, e.g., for aviation. For larger visibility values the difference is not so important.

The next two figures illustrate the correlations between measured and computed visibilities with (JANMODSZ in *Fig. 6*) and without (JANSSI *Fig. 7*) the use of decision tree procedure. High correlation (0.83) was reached with the

more developed method, as opposed to the low correlation (0.40) received applying only the simple FOGSI index (Eq. (4)). According to our experiences, the described decision tree procedure improves the results in all cases.

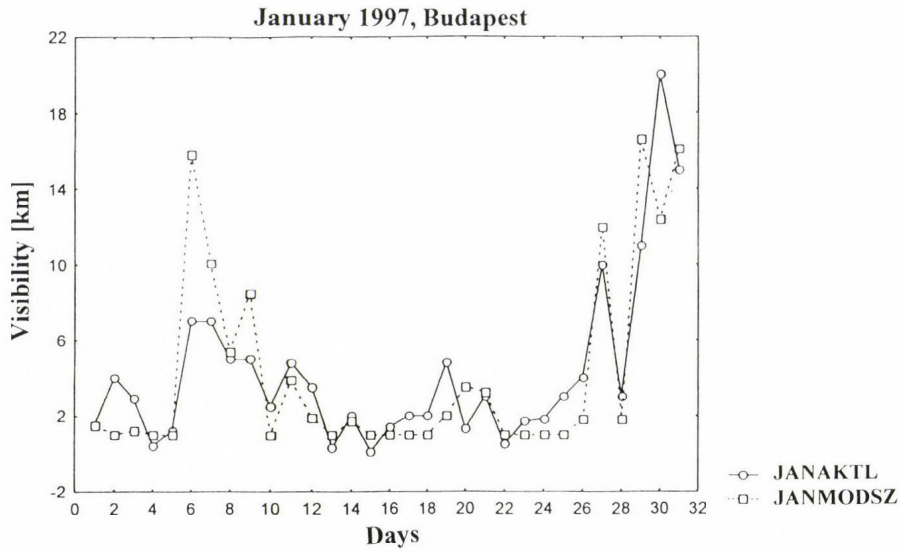

Fig. 5. Observed and diagnosed visibility.

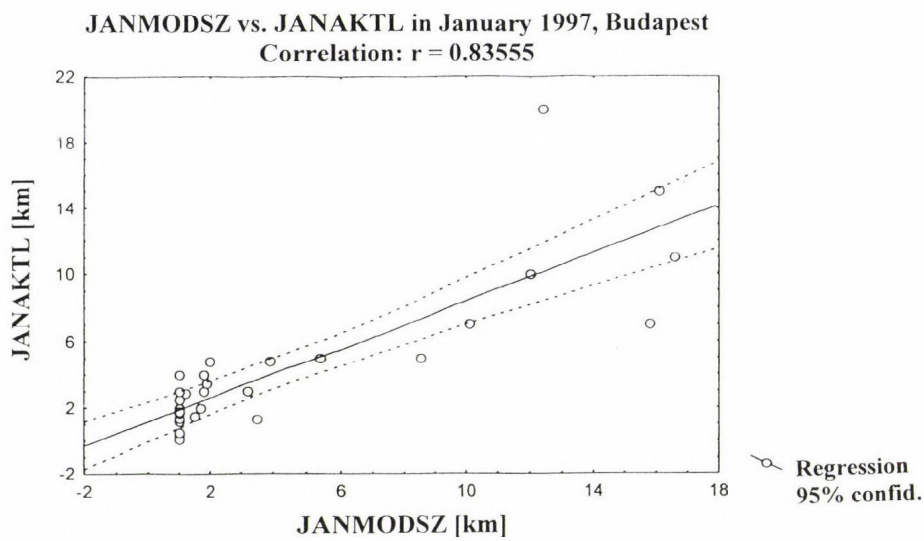

Fig. 6. Correlation between observed and calculated visibility using the decision tree.

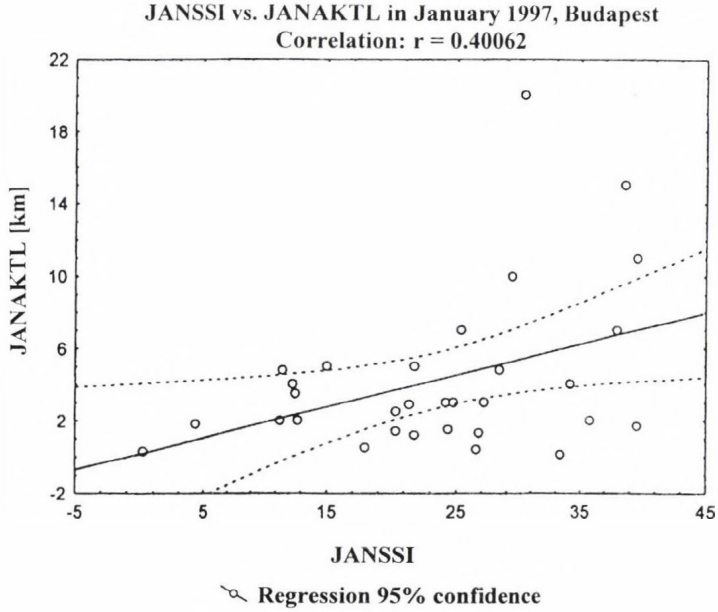

Fig. 7. Correlation between observed and diagnosed visibility.

An even more illustrative picture is presented in *Fig. 8*, where one can follow the hour by hour (continuos line) changes of real visibility compared to the 48-hour forecasts (columns). The run of observed and predicted visibility values is comparable to each other, although at some hours long shift might be detected. Regression coefficients were calculated based on the radiosounding data of Budapest and used for Szeged. It can be concluded, that Eq. (5) is adequate for most of the places of Hungary. A possible explanation is, that it is due to the relatively smooth surface of the country.

5. Conclusion

The described method is mainly used in aeronautical meteorology. After the test period this method was installed at the HMS Weather Forecasting and Aviation Meteorology Department. According to 3 years long experience, efficiency of the method strongly depends on the quality of the ALADIN model output near the ground level.

Another application area is nowcasting, where the application of the above outlined procedure for fog formation and dissipation, as well as the horizontal visibility led to significant improvements.

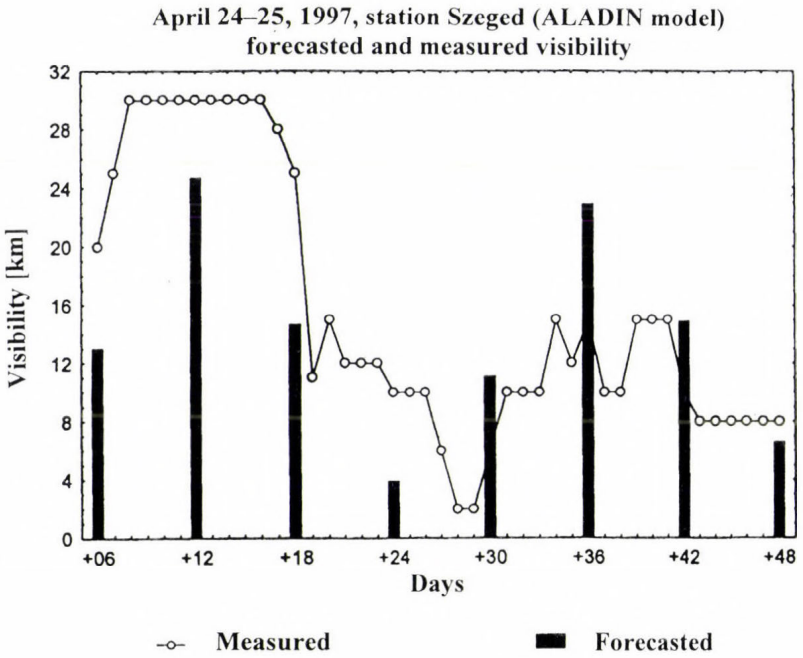

Fig. 8. Predicted and observed visibility in Szeged.

References

Bóna, M., 1986: Aerosynoptical research of cold air pad (in Hungarian). *Meteorológiai Tanulmányok*, No. 54, Országos Meteorológiai Szolgálat, Budapest.

Horányi, A., Ihász, I. and *Radnóti, G.*, 1996: ARPEGE/ALADIN: A numerical weather prediction model for Central-Europe with the participation of the Hungarian Meteorological Service. *Időjárás 100*, 277-301.

ICAO, 1998: *International Standards and Recommended Practices, Meteorological Service for International Air Navigation To the Convention on International Civil Aviation*. Thirteenth edition.

Kerényi, J., G. Szenyán, I., Putsay, M. and *Wantuch, F.*, 1995: Cloud detection on treshold technique for NOAA-AVHRR images for the Carpathian Basin. *Proc. of 1995 Meteorological Satellite Data Users' Conference*. Winchester, United Kingdom, 4-8 Sep 1995, 565-569.

Kilpinen, J., 1992: The application of Kalman filter in statistical interpretation of numerical weather forecasts. *12th Conference on Probability and Statistics in the Atmospheric Sciences*, June 22-26, 1992, Toronto, Ont., Canada, 11-16.

Pasini, A., Pelino, V. and *Potestà, S.*, 1999: A Neural Network model for visibility nowcasting from surface observations: results and sensitivity to physical input variables. Submitted to *Journal of Geophysical Research, D.*

Stessel, J.-P. and *Ottoy, H.*, 1999: Dense fog forecasting with an interactive expert. In *COST-78 Project II. 3, Final Report. Fog and Low Clouds: Statistical Methods and Decision Support Systems for Fog and Low Cloud Forecasting.*

Tóth, P., 1984.: Parameterization in the analysis of cold air pad forming and dissipation (in Hungarian). *Meteorológiai Tanulmányok*, No. 51. Országos Meteorológiai Szolgálat, Budapest.

IDŐJÁRÁS

Quarterly Journal of the Hungarian Meteorological Service
Vol. 105, No. 1, January–March 2001, pp. 39–58

Splitting method and its application in air pollution modeling

Ágnes Havasi[1], **Judit Bartholy**[1] and **István Faragó**[2]

[1]*Department of Meteorology, Eötvös Loránd University*
P.O. Box 32, H-1518 Budapest, Hungary
E-mails:hagi@nimbus.elte.hu; bari@nimbus.elte.hu

[2]*Department of Applied Analysis, Eötvös Loránd University,*
Kecskeméti u. 10, H-1053 Budapest, Hungary

(Manuscript received 1 August 2000; in final form 15 December 2000)

Abstract—The problems concerning the numerical solution of the chemistry-transport equations — the basis of all air pollution models — and the operator splitting procedure are discussed. The main aim of the paper is to clarify the mathematical background of operator splitting. The connection between Lie-algebra and the splitting procedure with its error (the so-called splitting error) is studied. Two important examples of the splitting technique are introduced (DEM splitting, physical splitting).

Key-words: air pollution problem, chemistry-transport equations, operator splitting, Lie-algebra.

1. Introduction

Nowadays air pollution is among the major environmental problems, especially in the developed industrial regions of the world. A considerable part of the total pollutant concentration emitted into the atmosphere is of anthropogenic origin. Recently atmospheric chemistry becomes one of the key disciplines of our understanding of air pollution and climatic processes. In 1995 Crutzen did win the Nobel Prize for chemistry for research results on this issue (*Crutzen* and *Zimmermann*, 1991; *Crutzen*, 1995; *Möller*, 1999). Approximately 20 billion tons of carbon-dioxide are discharged into the air every year solely due to the combustion of fossil fuels. Carbon-dioxide is the major anthropogenic greenhouse gas, therefore its increasing amount will probably lead to the warmth of the global climate in the forthcoming decades. Continuous monitoring of atmospheric CO_2 at Mauna Loa Observatory, Hawaii (*Keeling et al.,* 1989) indicates that the concentration of CO_2 gas has increased by about 26 percent over the pre-industrial level. With sophisticated climate model simulations we do have several climate

scenarios for the next 100 years, but on the base of some new findings by *Broecker* (1987) some are questionable. Hard to estimate the role of the ocean conveyor circulation (*Broecker*, 1991), but many evidences are available on its existence. Radiocarbon measurements of the GEOSECS programme imply that the conveyor circulation of the ocean could impact temporal changes in the $^{14}C/^{12}C$ ratio for atmospheric CO_2. Another important greenhouse gas is the tropospheric ozone, which is harmful not only to plants and animals, but also to human health. This gas is created from nitrogen-oxides and volatile organic compounds; all being dangerous toxic species. Another example is the discharge of toxic heavy metals (e.g., lead), which can get into the cycle of nutrients, so damaging the living organisms.

Reducing the emissions of the air pollutants is an important task, which requires international efforts (*Houghton*, 1995), since the high concentration values are not limited to the areas where the emission sources are located. First of all it is necessary to determine those critical concentration values, which should not be exceeded. The critical level for a given pollutant is the highest concentration value that will not cause damage to biological systems. (It is not reasonable to reduce the concentrations too much below critical levels, because the extra efforts may be very expensive and could cause economical difficulties.) Taking into account the critical levels, we have to work out control strategies on exactly where and how to reduce the emissions.

In the solution of the problem sketched above, the most efficient tools are the so-called chemistry-transport models. The development of such models is necessarily an intensive procedure requiring sensitivity studies of model components as well as validation against observations. The models are based on the mass conservation law, which is expressed in the form of a system of partial differential equations: the so-called (chemistry-)transport equations. To find the analytical solution of these equations is practically impossible, therefore we use some numerical method. However, the numerical treatment of the global problem is rather complicated. (Approximations of differential operators of different types, huge coupled discretized systems, etc.) That is why we apply a decoupling procedure, the so-called splitting technique. The point of this method is as follows. The original system of differential equations describes different processes (e.g., advection diffusion, etc.) that act simultaneously in the atmosphere. We replace this model with one in which appropriately chosen groups of these processes take place successively in time. This allows us to solve a few simpler systems instead of the whole one. However, the application of operator splitting usually implies some error, the so-called splitting error. The mathematical background of this error has not yet been completely clarified. The main aim of the paper is to introduce the technique of operator splitting and make clear both the background and the role of the splitting error.

In this article first we discuss the basic questions concerning the numerical treatment of the chemistry-transport equations. In Chapter 2 we introduce the

two basic approaches that can be applied in the numerical solution of this system: the Eulerian and the Lagrangian approach. In Chapter 3 we consider the basic questions related to the numerical solution of partial differential equations in general. In Chapter 4 we point out that some of the arising difficulties can be avoided by applying the useful technique of operator splitting. In the last three chapters we clarify the mathematical background and the role of operator splitting. First we investigate the splitting procedure on the simple problem of linear, constant coefficient systems. In Chapter 5 we move on to the more general case of linear operators. Here we describe the connection between Lie-algebras and Lie-groups, which serves as the mathematical background of operator splitting. Finally, in Chapter 7 we deal with the non-linear case, which, by the use of the Lie-operator formalism, leads back to the results of the previous chapter. Also, we formulate some conditions under which the splitting error vanishes.

2. The transport equations

Atmospheric transport of air pollutants is, in principle, a well-understood process (*Trenberth,* 1992). Assume that the concentration changes of m different chemical species are to be studied. Let $\mathbf{c}$ denote the vector in $\mathbf{R}^m$ containing the m concentration values. (In general, $\mathbf{c}$ may vary in space and time, so $\mathbf{c} = \mathbf{c}(\mathbf{x},t)$). If $\mathbf{u} = \mathbf{u}(\mathbf{x},t)$ denotes the three-dimension velocity vector, and c is the concentration of any of the m species then the changes of c can be described mathematically by the partial differential equation (PDE)

$$\frac{\partial c}{\partial t} + \nabla(\mathbf{u}c) = \nabla(\mathbf{K}\nabla c) + R(\mathbf{x},\mathbf{c}) + E + \sigma c \tag{1}$$

with the corresponding initial and boundary conditions. The m equations are coupled through the function $R(\mathbf{x},\mathbf{c})$ and so form a system of PDE's.

The different terms in the system (1) have the following physical meaning:

- The second term on the left-hand side describes the transportation due to the velocity field and is called the advection term. Advection transport plays an important role in the evolution of air pollutants and therefore appears in almost all air pollution models.
- The first term on the right-hand side expresses the turbulent diffusion. Here $\mathbf{K} = \mathbf{K}(\mathbf{x},t)$ is the so-called diffusion coefficient matrix.
- Term $R(\mathbf{x},\mathbf{c})$ represents the chemical reactions that take place during the atmospheric transport of the pollutants. The reactions included in air pollution models are usually of first and second order; in the latter case the vector function R is quadratically non-linear. The coefficients of the linear and the quadratic chemical terms express the rate at which the reactions proceed. The rates

of the different reactions can vary by several orders of magnitude, therefore the lifetime of the species can range from microseconds (e.g., hydrogen atoms) to centuries (e.g., nitrous oxide molecules).

- Term E expresses the emission, that is the discharge of the pollutants into the air either by natural (e.g., volcanic eruption of forest fires) or anthropogenic sources (e.g., urban traffic or combustion of fossil fuels).
- Finally, the residual σc term describes the deposition process, that is the removal of the pollutant particles from the air. We distinguish two basic types of deposition: wet and dry deposition. Wet deposition — or in other words precipitation scavenging — means removal of the particles by any kind of falling precipitation. Dry deposition includes gravitational sedimentation (particularly efficient for large particles), impaction on vegetation and absorption or reaction processes on the surface of the earth.

The above system of PDE's will simply be referred to as chemistry-transport (or simply transport) equations in the sequel (*Zlatev*, 1995). If we were able to solve the system (1) analytically, we could forecast the spatial and temporal changes of the continuous concentration fields. However, to find the analytical solution is practically impossible, unless some very unrealistic assumptions are made. The system is so complicated that we cannot even guarantee the existence of the unique solution, except in very special cases. The major difficulties are the following: (1) the reaction term $R(\mathbf{c})$ is usually non-linear; (2) the coefficients $\mathbf{u}$, $\mathbf{K}$ and σ are not constant and not necessarily continuous. Therefore in the sequel we assume the existence of the unique solution, which is a reasonable assumption because the model adequately describes the physics of air pollution transport. In the absence of any tools to obtain the analytical solution, the system must be treated numerically.

There are two main approaches that can be applied in the numerical treatment of the system (1). The first one is the so-called Eulerian approach, which is based on the following conception. A grid is defined on the space domain of interest, and the spatial derivatives in the system are discretized over the grid. As a result of the spatial discretization, we obtain an ordinary differential equation (ODE) at each gridpoint P_i (and for each chemical species) for the unknown time-depending function $c_d^i(t)$ approximating the concentration at the given point. (This procedure is called semi-discretization.) The obtained system of ODE's with the corresponding initial values is then solved numerically.

In the other approach — the so-called Lagrangian approach — the system of PDE's is simplified to a system of ODE's in the following way. Let us suppose that the wind components $u(x,y,t)$ and $v(x,y,t)$ are known, neglect the third velocity component w and consider a pollutant parcel in the spatial point (x_0,y_0) at time t. It is assumed that there is no diffusion, and the parcel as one piece is transported by the wind. This allows us to reduce the dimension of the problem. The trajectory of the parcel can be determined by solving the

$$\frac{dx}{dt} = u(t), \quad x(0) = x_0, \qquad \frac{dy}{dt} = v(t), \quad y(0) = y_0 \tag{2}$$

initial value problem. Our aim is to describe the concentration changes of the parcel along the trajectory. The concentration is influenced by chemical reactions, emission and deposition taking place along the trajectory. So the system

$$\frac{dc}{dt} = R(\mathbf{x},\mathbf{c}) + E(x(t), y(t), t) + \sigma c(x(t), y(t), t) \tag{3}$$

with the known functions $x(t)$, $y(t)$ is to be solved, which is a system of ODE's with the unknown function c depending only on time now. In practice, the system of Eqs. (2) and (3) can be solved numerically for example in the following steps:

- we discretize the time interval [0,T] using some Δt timestep,
- we solve the system (2) applying some numerical method (usually of Runge–Kutta type), and
- along the trajectory that we obtained numerically in the previous step, we solve the system (3).

In the solution of the two systems we should work with matching timesteps. We remark that the numerical method is not usually the same in the two cases. The system (2) is of very simple type, and it can even be solved by an explicit method. However, the system (3) is a so-called stiff system (because of the nonlinear $R(\mathbf{x},\mathbf{c})$ term), which means that stability may impose a restriction to the choice of the timestep. In the case of a stiff system, we should apply a so-called A-stable method, which allows us to choose an arbitrary timestep, that is in the choice of the timestep only accuracy and not stability accounts.

Both kinds of modeling have advantages as well as disadvantages. The main benefit of the Eulerian models is the use of the original equations describing all important physical processes that take place during the air pollution transport. Eulerian models perform better than Lagrangian ones

- if there are many emission sources;
- if all chemical reactions are taken into account during the transport; and
- if the air pollution transport is considered on a long time-scale.

However, running an Eulerian model is usually very expensive because of the high resolution. In addition to this, Eulerian models have problems with a strong single source resulting in sharp concentration gradients. An example of an Eulerian model is MEDIA, which was developed at the French Weather Service in 1990 and has been used operationally since 1998 at the Hungarian Meteorological Service (HMS) as well. The model was first validated on the Chernobyl re-

lease (*Piedelievre et al.,* 1990) and was successfully used among others in the case of the Algeciras nuclear accident (Spain) in May, 1998.

On short-scale and in the case of a single source, the use of a Lagrangian model is usually more advantageous. The system of ODE's obtained along the trajectories is easier to treat numerically than the original system of PDE's. Due to the simple conception, the results of a Lagrangian model are easier to interpret. These models are good for experimental purposes and they are especially useful when the origin of the pollutant is to be determined. To this end so-called backward trajectories are calculated, that is the pathway of the pollutant parcel is computed backward in time. A report on the application of a Lagrangian model can be found in *Eliassen et al.* (1982), where a Norwegian case study is analysed, and it is pointed out that the high Scandinavian ozone levels are not due to Scandinavian sources but probably to emissins of primary pollutants in Eastern Europe. For other applications of Lagrangian models see also *Olson et al.* (1992) and *Simpson* (1992, 1993).

The major disadvantage of Lagrangian models is the low accuracy, especially distant to the source, because of the ignorance of the diffusion and the exponential increase of errors in the trajectory calculations. In some situations the combination of a Lagrangian and an Eulerian model may be the best choice, e.g., when the long-range transport of pollutants discharged by a sharp single source (such as an accidental release from a nuclear power plant) is to be studied. In this case it is advisable to apply a Lagrangian model near the source, but from a certain distance it is better to switch over to an Eulerian one. A critical point of this procedure is the coupling of the two models at the boundary of the Lagrangian and the Eulerian domain (*Brandt et al.*, 1998).

The numerical treatment of the system of PDE's (1) is not a simple problem. In the next chapter we consider the main aspects of selecting a proper numerical method for solving the system (1).

3. Numerical solution of the transport equations

The numerical solution of the system of PDE's (1) is based on defining a mesh sequence on the domain of the system. Discretization of the model equations over the meshes leads to a discrete model sequence. We determine a numerical solution on each mesh. It is also necessary to define a measure (or norm) of the elements on each mesh, which can be, for example, the maximum of the grid-point values or the square sum. Of course, when realising the numerical method, we cannot work with the infinite mesh sequence, but we stop after a finite number of steps. (We use a so-called stopping criterion. For example we stop when the difference between the numerical solutions following one another is sufficiently small. For details see *Marchuk* (1980) and *Thomée* (1990)). In the fol-

lowing we turn our attention to the questions concerning the numerical solution obtained as above.

• **Efficiency.** The discretization of the system leads to a huge computational problem, especially in the case of Eulerian models. Therefore it is crucial to perform efficiently the most time-consuming calculations in the numerical solution.

• **Consistency.** The exact solution of the continuous model does not usually satisfy the discrete model equations. We introduce the notion of the local error to measure how well the exact solution satisfies the numerical model. The local error of one discrete model in the model sequence is the quantity obtained by substituting the exact solution into the discrete model. The method is called consistent if the local error in the discrete model sequence tends to zero, that is in limit the exact solution satisfies the discrete model.

• **Stability.** We expect the numerical method to be stable, which means that for all input data the numerical solution in absolute value remains under a bound. This is important because the input data usually come from measurements and go through some data-processing procedures (e.g., interpolation on the grid) and, therefore, unavoidably contain errors. In the case of certain methods, a relation between the spatial and the temporal stepsize (a so-called stability criterion) has to be fulfilled so that the method is stable. In practice this means a limitation for the choice of the timestep-size at a given spatial stepsize. It is most advantageous if the method is unconditionally stable, i.e., there is no restriction for stability. We remark that the notion of stability is norm-dependent.

• **Convergence.** The approximation is called convergent if the difference between the exact and the numerical solution in the discrete model sequence (the so-called global error) tends to zero. Convergence is closely related to stability according to Lax's equivalence theory, which roughly says that in the case of consistency stability is a necessary and sufficient condition for convergence.
Obviously, the speed of the convergence is also of great importance, since in practice the timestep-size cannot be chosen to be arbitrarily small.

• **Preservation of main qualitative properties.** Some methods satisfy all the above requirements, however, the numerical solution is not acceptable, because it does not preserve some basic qualitative property of the exact solution. Suppose that the numerical solution is convergent, and the exact solution at a given point is a small positive concentration value. It can happen that though the numerical solution tends to this positive value, in the case of the given mesh it gives a negative value at this point. This should be avoided because (1) negative concentration values have no physical meaning, and (2) the physically impossible values can cause difficulties when these are used as input data in another model.

A further important qualitative property is the preservation of the shape of the exact solution (e.g., convexity, monotonicity). From a physical point of view, an especially important qualitative property is mass conservation. The transport equations express a fundamental physical law: the local change of the concentration at a point is equal to the amount that is transported to that point by

different transport processes. However, this physical principle can be broken when the continuous equations are discretized, which leads to unrealistic results. Stability in an arbitrary norm is not usually sufficient for the preservation of the above properties, but roughly speaking, stability in the maximum norm is already enough in most cases.

We remark that though so far we have focused on the qualitative properties of the exact solution of the continuous model, the ultimate aim of modeling is to describe the behaviour of a physical system. In some cases the exact solution of the continuous model does not reflect the real behaviour of the physical system. For example, the analytical solution of the heat equation results in an infinite velocity of heat, which contradicts any experience. However, certain numerical methods do not have this bad property, so the numerical solution may even improve the continuous model. (More details for a special heat equation can be found in *Faragó et al.* (1993)).

The above requirements are natural, and it is highly desirable to satisfy all of them simultaneously when solving numerically the transport equations. However, this is not a simple task. Since the terms on the right-hand side have different properties, the system is too complicated and theoretical results are not applicable. Therefore, it is impossible to satisfy all the requirements simultaneously, if we apply direct approximation to the system. A possible approach to the solution of this problem is operator splitting, which will be introduced in the next chapter.

4. Operator splitting

Operator or time splitting is commonly used in air pollution modeling. The basic idea behind this procedure is dividing the spatial differential operator of the system (1) into a few simpler operators, and solving the corresponding systems — which are connected to each other through the suitable initial conditions — successively in each timestep (*Marchuk,* 1988; *Yanenko,* 1962; *Lanser* and *Verwer*, 1999).

Operator splitting is usually applied according to the different physical processes involved in the model. As an example, we introduce the splitting procedure of the Danish Eulerian Model (DEM). In this long-range air pollution model, the splitted sub-systems describe the horizontal advection (Eq. (4)), the horizontal diffusion (Eq. (5)), the chemical reactions with the emission (Eq. (6)), the deposition (Eq. (7)) and the vertical exchange (Eq. (8)).

$$\frac{\partial c^{(1)}}{\partial t} = -\frac{\partial (uc^{(1)})}{\partial x} - \frac{\partial (vc^{(1)})}{\partial y} \tag{4}$$

$$\frac{\partial c^{(2)}}{\partial t} = \frac{\partial}{\partial x}\left(k_1 \frac{\partial c^{(2)}}{\partial x}\right) + \frac{\partial}{\partial y}\left(k_2 \frac{\partial c^{(2)}}{\partial y}\right) \tag{5}$$

$$\frac{\partial c^{(3)}}{\partial t} = E + R(\mathbf{c}^{(3)}) \tag{6}$$

$$\frac{\partial c^{(4)}}{\partial t} = \sigma c^{(4)} \tag{7}$$

$$\frac{\partial c^{(5)}}{\partial t} = -\frac{\partial (w c^{(5)})}{\partial z} + \frac{\partial}{\partial z}\left(k_3 \frac{\partial c^{(5)}}{\partial z}\right). \tag{8}$$

In the above splitting procedure, the original system of PDE's has been split into five simpler systems, which are to be solved in each timestep one after the other in the following way. Assume that some approximation to the concentration vector **c** at time t has been found. The first system is solved by using this vector as a starting vector. The obtained solution will serve as the initial vector in the treatment of the second system and so on. The solution of the fifth system is accepted as an approximation to the concentration vector at the end of the timestep.

Operator splitting has several advantages:

- The splitted sub-systems are easier to treat numerically than the original system.
- We can exploit the special properties of the different sub-systems and apply the most suitable method for each.
- If each method is stable and preserves the main qualitative properties then so does the global model.

It is obvious that this kind of de-coupling procedure may cause inaccuracy in the solution. This is called splitting error, which will be described in more details in the next chapters.

5. Investigation of splitting method on a simple problem

First let us consider the simple linear, constant coefficient system

$$\frac{d\mathbf{w}}{dt} = \mathbf{A}\mathbf{w}(t) + \mathbf{B}\mathbf{w}(t) \tag{9}$$

with the initial condition

$$\mathbf{w}(0) = \mathbf{w}_0,$$

where $\mathbf{w}$: $\mathbf{R} \rightarrow \mathbf{R}^n$ is the unknown vector function, and $\mathbf{A}$ and $\mathbf{B}$ are matrices of type $\mathbf{R}^{n \times n}$. The exact solution of the above initial value problem at a time τ is

$$\mathbf{w}(\tau) = e^{(\mathbf{A}+\mathbf{B})\tau}\mathbf{w}_0. \tag{10}$$

Now let us split the problem into the following two simpler problems:

$$\left.\begin{aligned} \frac{d\mathbf{w}^{(1)}}{dt} &= \mathbf{A}\mathbf{w}^{(1)}(t) \\ \mathbf{w}^{(1)}(0) &= \mathbf{w}_0 \end{aligned}\right\} \tag{11}$$

and

$$\left.\begin{aligned} \frac{d\mathbf{w}^{(2)}}{dt} &= \mathbf{B}\mathbf{w}^{(2)}(t) \\ \mathbf{w}^{(2)}(0) &= \mathbf{w}^{(1)}(\tau) \end{aligned}\right\}. \tag{12}$$

The solution of the first system at time τ is

$$\mathbf{w}^{(1)}(\tau) = e^{\mathbf{A}\tau}\mathbf{w}_0\,, \tag{13}$$

which is applied as the initial value for the second system. So the exact solution of the splitted problem at time τ is

$$\mathbf{w}_{Sp}(\tau) = \mathbf{w}^{(2)}(\tau) = e^{\mathbf{B}\tau}e^{\mathbf{A}\tau}\mathbf{w}_0\,. \tag{14}$$

The splitting error is defined as the difference between (10) and (14), that is

$$Err_{Sp} := \mathbf{w}(\tau) - \mathbf{w}_{Sp}(\tau) = e^{(\mathbf{A}+\mathbf{B})\tau}\mathbf{w}_0 - e^{\mathbf{B}\tau}e^{\mathbf{A}\tau}\mathbf{w}_0\,. \tag{15}$$

Clearly, for any initial vector, the splitting error is zero if and only if the equality

$$e^{(\mathbf{A}+\mathbf{B})\tau} = e^{\mathbf{B}\tau}e^{\mathbf{A}\tau} \tag{16}$$

holds. Let us compare the two sides. According to the definition of the matrix exponential

$$e^{(\mathbf{A}+\mathbf{B})\tau} = \mathbf{I} + (\mathbf{A}+\mathbf{B})\tau + \frac{1}{2!}(\mathbf{A}+\mathbf{B})^2\tau^2 + o(\tau^3) =$$

$$= \mathbf{I} + (\mathbf{A}+\mathbf{B})\tau + \frac{1}{2!}(\mathbf{A}^2+\mathbf{B}^2)\tau^2 + \frac{1}{2!}(\mathbf{AB})\tau^2 + \frac{1}{2!}(\mathbf{BA})\tau^2 + o(\tau^3) \tag{17}$$

and

$$e^{\mathbf{B}\tau}e^{\mathbf{A}\tau} = (\mathbf{I} + \mathbf{B}\tau + \frac{1}{2!}\mathbf{B}^2\tau^2 + o(\tau^3))(\mathbf{I} + \mathbf{A}\tau + \frac{1}{2!}\mathbf{A}^2\tau^2 + o(\tau^3)) =$$

$$= \mathbf{I} + \mathbf{A}\tau + \frac{1}{2!}\mathbf{A}^2\tau^2 + \mathbf{B}\tau + \mathbf{BA}\tau^2 + \frac{1}{2!}\mathbf{B}^2\tau^2 + o(\tau^3) =$$

$$= \mathbf{I} + (\mathbf{A} + \mathbf{B})\tau + \frac{1}{2!}(\mathbf{A}^2 + \mathbf{B}^2)\tau^2 + \mathbf{BA}\tau^2 + o(\tau^3). \tag{18}$$

It is seen that the terms of order $o(\tau^2)$ in the expression of the error vanish if

$$\frac{1}{2}\mathbf{AB} + \frac{1}{2}\mathbf{BA} = \mathbf{BA},$$

that is if

$$\mathbf{AB} = \mathbf{BA},$$

or in other words, the matrices **A** and **B** commute. It is easy to see that in case the matrices **A** and **B** do not commute, then the splitting error is of $o(\tau^2)$. Furthermore, provided that the matrices commute, the difference resulting from the higher order terms in Eqs. (17) and (18) also turns into zero, that is there is no splitting error. The proof of this assertion will be given for the more general case of linear operators in the following chapter.

6. Splitting for linear operators

In the remaining two chapters we will consider operators of type S $\rightarrow$ S, where S is a normed space of functions. In this space we can define the composition in the usual sense, that is for any $\mathbf{C}_1$, $\mathbf{C}_2$: S$\rightarrow$S $(\mathbf{C}_1 \circ \mathbf{C}_2)(x)$ means $\mathbf{C}_1(\mathbf{C}_2(x))$. First we have to introduce the notion of the operator exponential, since it will play an important role in our investigations. Let **C** be an operator mapping from S to S. Suppose that the series

$$\mathbf{I}(x) + \frac{1}{1!}\mathbf{C}(x) + \frac{1}{2!}(\mathbf{C} \circ \mathbf{C})(x) + \frac{1}{3!}(\mathbf{C} \circ \mathbf{C} \circ \mathbf{C})(x) + \cdots \tag{19}$$

is convergent to an element $x^* \in$ S for all $x \in$ H $\subset$ D(**C**). (Here the letter I stands for the identity operator of type S$\rightarrow$S.)

Definition: The operator $e^{\mathbf{C}}$: $x \rightarrow x^*$, D($e^{\mathbf{C}}$):= H is called the exponential of the operator **C**.

In this chapter we restrict our attention to linear problems, that is we consider the system

$$\frac{d\mathbf{w}}{dt} = \mathbf{L}_1\mathbf{w}(t) + \mathbf{L}_2\mathbf{w}(t) \tag{20}$$

with the initial condition

$$\mathbf{w}(0) = \mathbf{w}_0.$$

Here $\mathbf{w} \in S$ is the unknown function, and $\mathbf{L}_1$, $\mathbf{L}_2$ on the right-hand side denote two linear operators of type S→S. The splitted subproblems have the form

$$\left.\begin{aligned} \frac{d\mathbf{w}^{(1)}}{dt} &= \mathbf{L}_1\mathbf{w}^{(1)}(t) \\ \mathbf{w}^{(1)}(0) &= \mathbf{w}_0 \end{aligned}\right\} \tag{21}$$

and

$$\left.\begin{aligned} \frac{d\mathbf{w}^{(2)}}{dt} &= \mathbf{L}_2\mathbf{w}^{(2)}(t) \\ \mathbf{w}^{(2)}(0) &= \mathbf{w}^{(1)}(\tau) \end{aligned}\right\}. \tag{22}$$

As we mentioned before, we assume that both the original problem and the splitted subproblems have a unique solution. It is known (see for example *Engel* and *Nagel* (2000)) that in this case the solution can be given again with the help of exponentials. Namely, the solution of the first splitted subsystem at time τ is

$$\mathbf{w}^{(1)}(\tau) = e^{\mathbf{L}_1\tau}\mathbf{w}_0, \tag{23}$$

and the exact solution of the whole splitted problem at time τ has the form

$$\mathbf{w}_{Sp}(\tau) = \mathbf{w}^{(2)}(\tau) = e^{\mathbf{L}_2\tau}\, e^{\mathbf{L}_1\tau}\mathbf{w}_0. \tag{24}$$

It is seen that the error of the splitting procedure is related to the difference between the expressions $e^{\mathbf{L}_2\tau}\, e^{\mathbf{L}_1\tau}$ and $e^{(\mathbf{L}_1+\mathbf{L}_2)\tau}$, similarly to the case of the matrices. The splitting error vanishes for all initial functions $\mathbf{w}_0$ if and only if $e^{\mathbf{L}_2\tau}\, e^{\mathbf{L}_1\tau} = e^{(\mathbf{L}_1+\mathbf{L}_2)\tau}$. This equality expresses that the product of $e^{\mathbf{L}_2\tau}$ and $e^{\mathbf{L}_1\tau}$ can be obtained by applying the exponential function to the sum $\mathbf{L}_1\tau + \mathbf{L}_2\tau$. The following questions arise naturally:

(1) What is the condition of the equality?

(2) If the equality does not hold, then, instead of the exponential function, what kind of function (if such exists) connects the product and the sum?

To formulate this connection, we will need the notions of Lie-algebra and Lie-group. Let $(V, +, \cdot)$ be a vector space (in the usual sense) and $[\cdot, \cdot]: V \times V \to V$ an additional operation called commutation with the following properties:

(1) $[\lambda_1 X_1 + \lambda_2 X_2, Y] = [\lambda_1 X_1, Y] + [\lambda_2 X_2, Y]$,

(2) $[X, Y] = -[Y, X]$,

(3) $[X,[Y,Z]] + [Y,[Z,X]] + [Z,[X,Y]] = 0$

for all X, X_1, X_2, Y, Y_1, Y_2 and $Z \in V$. The first property is called bilinearity, the second one is the scew-symmetry and the third one is the so-called Jacobi-identity. $[X, Y]$ is called the commutator of the elements X and Y.

It is easy to check that provided a natural product $(X, Y) \to Y$ exists between the elements of the vector space V, then with the operation

$$[X, Y] := XY - YX, \quad X, Y \in V$$

the vector space V forms a Lie-algebra. Particularly, if V is identified with a function space, then we can define this natural product of X and Y in V as the function composition $X \circ Y$. Therefore, the operation

$$[X, Y] := X \circ Y - Y \circ X$$

determines a Lie-algebra.

In the case when a natural product exists on the vector space V, we can define the exponentials of the elements of V. Let L denote the exponentials of those elements of V, for which their exponential exists. Let us provide this set of exponentials with an appropriate product between the elements to obtain a group L. If $V \equiv \mathrm{Hom}(S)$ (linear operators of type $S \to S$), then the exponentials of the elements are operators of type $S \to S$, and the composition of these exponential operators is a group product. It is important that in our case the vector space Hom(S) with the induced operator norm is topological (because it is a normed space), therefore the above group of exponentials forms a so-called Lie-group. The connection between a Lie-algebra and its Lie-group is expressed by the following theorem (see *Varadarajan*, 1974).

Theorem. (Baker–Campbell–Hausdorff-formula) Let $(V, [\cdot, \cdot])$ be a Lie-algebra, and L its Lie-group. Then for all X and Y in V and for any scalar t the product of e^{Xt} and $e^{Yt} \in L$ can be given in the form

$$e^{Xt} e^{Yt} = e^{\sum_{n=0}^{\infty} t^n c_n(X,Y)}, \tag{25}$$

where the functions $c_n(X,Y)$: $V \times V \to V$, $n = 1, 2, \ldots$ are obtained recursively as follows:

$$c_0(X,Y) = 0,$$

$$c_1(X,Y) = X + Y,$$

$$(n+1)\, c_{n+1}(X,Y) = \frac{1}{2}[X - Y, c_n(X,Y)]$$
$$+ \sum_{p \geq 1,\, 2p \leq n} K_{2p} \sum_{\substack{k_1, \ldots, k_{2p} > 0 \\ k_1 + \cdots + k_{2p} = n}} [c_{k_1}(X,Y), [\ldots [c_{k_{2p}}(X,Y), X + Y] \ldots]],$$

where $k_1, \ldots, k_{2p}$ are natural numbers, and $K_2, \ldots, K_{2p}$ are given constants. We remark that the coefficients $c_0(X,Y)$ and $c_1(X,Y)$ can be easily obtained by direct comparison of the series

$$e^{Xt} e^{Yt} = \left(I + Xt + \frac{1}{2!} X^2 t^2 + \ldots\right)\left(I + Yt + \frac{1}{2!} Y^2 t^2 + \ldots\right) = I + (X+Y)t + \ldots$$

and

$$e^{\sum_{n=0}^{\infty} t^n c_n(X,Y)} = I + \left(c_0 + c_1 t + \frac{1}{2!} c_2 t^2 + \ldots\right) + \frac{1}{2!}\left(c_0 + c_1 t + \ldots\right) + \ldots$$

We seek the condition of the equality

$$e^{Xt} e^{Yt} = e^{(X+Y)t}. \tag{26}$$

Comparing the right-hand sides of Eq. (25) and Eq. (26) we see that Eq. (26) holds if and only if $c_i(X,Y) = 0$ for all $i \geq 2$.

Substituting $n = 1$ into the recursive formula we obtain that

$$c_2(X,Y) = \frac{1}{2}[X,Y],$$

which means that

$$[X,Y] = 0 \tag{27}$$

is a necessary condition of the equality (26). Substituting greater values of n we see that if Eq. (27) holds then the coefficients $c_3(X,Y)$, $c_4(X,Y)$, etc., of the higher order terms also turn into zero. So, the equality (26) holds if and only if $[X,Y] = 0$.

This result is directly applicable to the splitting problem Eqs. (20) to (22), as follows. Let $V \equiv \mathrm{Hom}(S)$, and let us define the commutator of $\mathbf{L}_1$ and $\mathbf{L}_2$ in S as

$$[\mathbf{L}_1,\mathbf{L}_2] := \mathbf{L}_1 \circ \mathbf{L}_2 - \mathbf{L}_2 \circ \mathbf{L}_1.$$

In such a way we have obtained a Lie-algebra over the topological (normed) vector space Hom(S). As we pointed out earlier, the splitting error vanishes if and only if

$$e^{\mathbf{L}_2\tau}\, e^{\mathbf{L}_1\tau} = e^{(\mathbf{L}_1+\mathbf{L}_2)\tau}. \tag{28}$$

The expression on the right-hand side is the composition of the exponentials of $\mathbf{L}_2\tau \in \mathrm{Hom}(S)$ and $\mathbf{L}_1\tau \in \mathrm{Hom}(S)$. The set of the exponentials of the elements in Hom(S) provided with the composition operation forms a Lie-group. Therefore, according to our previous considerations, the equality (28) holds if and only if

$$[\mathbf{L}_1, \mathbf{L}_2] = 0,$$

which yields that the splitting error vanishes if and only if

$$\mathbf{L}_1 \circ \mathbf{L}_2 = \mathbf{L}_2 \circ \mathbf{L}_1.$$

7. Splitting for non-linear operators

In the general non-linear case the splitting error is related to the notion of L-commutativity. Let **F** and **G**: S→S be usually non-linear differentiable mappings. We define the operator $\mathbf{E}_{F,G}$: S→S as follows:

$$\mathbf{E}_{F,G}(s) := (\mathbf{G}'(s) \circ \mathbf{F})(s) - (\mathbf{F}'(s) \circ \mathbf{G})(s), \tag{29}$$

where ' refers to the derivative. (The operators **F**'(s) and **G**'(s) are in Lin(S), where Lin(S) denotes the space of continuous linear operators of type S→S.)

Definition: The operator $\mathbf{E}_{F,G}$ is called the commutator of the mappings **F** and **G**.

Definition: We say that the operators **F** and **G** L-commute if their commutator is zero, that is if $\mathbf{E}_{F,G} = 0$.

In the following we will show the connection between the L-commutativity and the splitting error with the help of the so-called Lie operator formalism.

Let us consider the general non-linear problem

$$\frac{\partial \mathbf{c}}{\partial t}(\mathbf{x},t) = \mathbf{F}(\mathbf{c}(\mathbf{x},t)), \tag{30}$$

where $\mathbf{c}(\mathbf{x},t)$ is vector-valued in $\mathbf{R}^m$, and $\mathbf{F}$ represents a usually non-linear operator. As before, we assume that the system has a unique solution $\mathbf{c}(\mathbf{x},t)$ and it is an analytical function. Then the Taylor-series expansion of the solution according to the variable t reads

$$\mathbf{c}(\mathbf{x},t+\tau) = \mathbf{c}(\mathbf{x},t) + \tau\frac{\partial \mathbf{c}}{\partial \mathbf{t}}(\mathbf{x},t) + \tau^2\frac{1}{2!}\frac{\partial^2 \mathbf{c}}{\partial t^2}(\mathbf{x},t) + \ldots + \tau^k\frac{1}{k!}\frac{\partial^k \mathbf{c}}{\partial t^k}(\mathbf{x},t) + \ldots \tag{31}$$

Substituting Eq. (30) into Eq. (31) we get the relation

$$\mathbf{c}(\mathbf{x},t+\tau) = \mathbf{c}(\mathbf{x},t) + \tau\mathbf{F}(\mathbf{c}(\mathbf{x},t)) + \tau^2\frac{1}{2!}\frac{\partial}{\partial t}\mathbf{F}(\mathbf{c}(\mathbf{x},t)) + \ldots + \tau^k\frac{1}{k!}\frac{\partial^{k-1}}{\partial \mathrm{t}^{k-1}}\mathbf{F}(\mathbf{c}(\mathbf{x},t)) + \ldots \tag{32}$$

Now with the given operator $\mathbf{F}$ we associate a new operator, which we will denote by $\hat{\mathrm{F}}$. This is the so-called Lie operator which acts on the space of the differentiable operators of type S→S and maps each operator $\mathbf{G}$ into the new operator $\hat{\mathrm{F}}(\mathbf{G})$, such that for any element $\mathrm{c} \in \mathrm{S}$

$$(\hat{\mathrm{F}}(\mathbf{G}))(\mathbf{c}) = (\mathbf{G}'(\mathbf{c}) \circ \mathbf{F})(\mathbf{c}). \tag{33}$$

It is easy to see that the Lie operator is linear. Applying the operator $\hat{\mathrm{F}}(\mathbf{G})$ to the element $\mathbf{c}(\mathbf{x},t)$ and using Eq. (30) and the well-known chain rule of differentiating, we obtain that

$$\begin{aligned}(\hat{\mathrm{F}}(\mathbf{G}))(\mathbf{c}(\mathbf{x},t)) &= (\mathbf{G}'(\mathbf{c}(\mathbf{x},t)) \circ \mathbf{F})(\mathbf{c}(\mathbf{x},t)) = (\mathbf{G}'(\mathbf{c}(\mathbf{x},t)))(\mathbf{F}(\mathbf{c}(\mathbf{x},t))) = \\ &= (\mathbf{G}'(\mathbf{c}(\mathbf{x},t)))(\frac{\partial \mathbf{c}}{\partial t}(\mathbf{x},t)) = \frac{\partial}{\partial t}\mathbf{G}(\mathbf{c}(\mathbf{x},t)).\end{aligned} \tag{34}$$

From induction follows that the k^{th} power of the Lie-operator $\hat{\mathrm{F}}$ applied to some operator $\mathbf{G}$ can be expressed as the k^{th} derivative of $\mathbf{G}$, that is the relation

$$(\hat{\mathrm{F}}^{\mathrm{k}}(\mathbf{G}))(\mathbf{c}(\mathbf{x},t)) = \frac{\partial^k}{\partial t^k}\mathbf{G}(\mathbf{c}(\mathbf{x},t)) \tag{35}$$

is valid for all $\mathrm{k} = 1, 2\ldots$.

Taking into account Eq. (32) and Eq. (35), for the function $\mathbf{c}(\mathbf{x},t)$ the relation

$$\mathbf{c}(\mathbf{x},t+\tau) = \mathbf{I}(\mathbf{c}(\mathbf{x},t)) + \frac{1}{1!}(\tau\hat{\mathrm{F}}(\mathbf{I}))\,(\mathbf{c}(\mathbf{x},t)) + \ldots + \frac{1}{k!}(\tau^k\hat{\mathrm{F}}^k(\mathbf{I}))\,(\mathbf{c}(\mathbf{x},t)) + \ldots =$$

$$= (\mathbf{I} + \frac{1}{1!}(\tau\hat{\mathrm{F}})\,(\mathbf{I}) + \ldots + \frac{1}{k!}(\tau^k\hat{\mathrm{F}}^k)\,(\mathbf{I}) + \ldots)\,(\mathbf{c}(\mathbf{x},t)) \equiv (e^{\tau\hat{\mathrm{F}}}(\mathbf{I}))\,(\mathbf{c}(\mathbf{x},t)) \qquad (36)$$

is valid, where the defining equality is right, because the series on the right-hand side is convergent.

Let us split the operator $\mathbf{F}$ into the sum $\mathbf{F_1} + \mathbf{F_2}$. From the above consideration follows that the splitting error is

$$\mathrm{Err}_{\mathrm{Sp}} = (e^{\tau(\hat{\mathrm{F}}_1+\hat{\mathrm{F}}_2)}(\mathbf{I}) - (e^{\tau\hat{\mathrm{F}}_2}\,e^{\tau\hat{\mathrm{F}}_1})\,(\mathbf{I}))\,(\mathbf{c}(\mathbf{x},t))\,. \qquad (37)$$

This error vanishes for all $\mathbf{c}(\mathbf{x},t)$ if and only if

$$e^{\tau(\hat{\mathrm{F}}_1+\hat{\mathrm{F}}_2)}(\mathbf{I}) = (e^{\tau\hat{\mathrm{F}}_2}\,e^{\tau\hat{\mathrm{F}}_1})\,(\mathbf{I})\,. \qquad (38)$$

At this point the previous results are again applicable. If we define the usual addition operation between the Lie-operators, that is

$$(\hat{\mathrm{F}}_1+\hat{\mathrm{F}}_2)\,(\mathbf{G}) := \hat{\mathrm{F}}_1(\mathbf{G}) + \hat{\mathrm{F}}_2(\mathbf{G})$$

and

$$(\lambda\hat{\mathrm{F}})\,(\mathbf{G}) := \lambda\hat{\mathrm{F}}(\mathbf{G}),$$

then the set of Lie-operators form a vector space. Moreover, defining the commutation operation by

$$[\hat{\mathrm{F}}_1,\hat{\mathrm{F}}_2] := \hat{\mathrm{F}}_1 \circ \hat{\mathrm{F}}_2 - \hat{\mathrm{F}}_2 \circ \hat{\mathrm{F}}_1,$$

we obtain a Lie-algebra. As $e^{\tau\hat{\mathrm{F}}_2}\,e^{\tau\hat{\mathrm{F}}_1}$ is given by the Baker–Campbell–Hausdorff-formula, therefore, for an operator $\mathbf{G}$ the relation

$$e^{\tau(\hat{\mathrm{F}}_1+\hat{\mathrm{F}}_2)}(\mathbf{G}) = (e^{\tau\hat{\mathrm{F}}_2}\,e^{\tau\hat{\mathrm{F}}_1})\,(\mathbf{G})$$

holds if and only if the equality

$$(\hat{\mathrm{F}}_1 \circ \hat{\mathrm{F}}_2)\,(\mathbf{G}) = (\hat{\mathrm{F}}_2 \circ \hat{\mathrm{F}}_1)\,(\mathbf{G})$$

is satisfied. We expect this equality to be valid only for the identity operator $\mathbf{I}$, that is we only need the equality

$$((\hat{F}_1 \circ \hat{F}_2)(\mathbf{I}))(\mathbf{c}) = ((\hat{F}_2 \circ \hat{F}_1)(\mathbf{I}))(\mathbf{c}) \tag{39}$$

to be satisfied for all $\mathbf{c} \in S$. Applying the definition of the Lie operator we can see that Eq. (39) is equivalent to the relation

$$(\mathbf{F}_1'(\mathbf{c}) \circ \mathbf{F}_2)(\mathbf{c}) = (\mathbf{F}_2'(\mathbf{c}) \circ \mathbf{F}_1)(\mathbf{c}) \tag{40}$$

for all $\mathbf{c} \in S$, which means that the operators $\mathbf{F}_1$ and $\mathbf{F}_2$ L-commute. If $\mathbf{F}_1$ and $\mathbf{F}_2$ do not commute, then the splitting error is of $o(\tau^2)$.

The condition (40) can be used to analyse the splitting error of a given splitting procedure. At the beginning of the chapter we introduced DEM splitting. An alternative procedure can be the splitting of the spatial differential operator on the right-hand side of the system (1) purely according to the physical processes, which means that we have the splitted operators

- $\mathbf{F}_1(\mathbf{c}) = -\nabla(\mathbf{uc})$ for the advection,
- $\mathbf{F}_2(\mathbf{c}) = \nabla(\mathbf{K}\nabla\mathbf{c})$ for the diffusion,
- $\mathbf{F}_3(\mathbf{c}) = \boldsymbol{\sigma}\mathbf{c}$ for the deposition,
- $\mathbf{F}_4(\mathbf{c}) = \mathbf{E}$ for the emission, and
- $\mathbf{F}_5(\mathbf{c}) = \mathbf{R}(\mathbf{c})$ for the chemistry.

Here for example the commutator of the advection and diffusion operators reads

$$\mathbf{E}_{1,2}(\mathbf{c}) = (\mathbf{F}_2'(\mathbf{c}) \circ \mathbf{F}_1)(\mathbf{c}) - (\mathbf{F}_1'(\mathbf{c}) \circ \mathbf{F}_2)(\mathbf{c}) = \nabla[\mathbf{K}\nabla(-\nabla(\mathbf{uc}))] + \nabla[\mathbf{u}(\nabla(\mathbf{K}\nabla\mathbf{c}))].$$

The L-commutativity of all pairs of operators in the physical splitting is analysed in details in *Dimov et al.* (1999). For example it is shown that provided the diffusion coefficient matrix $\mathbf{K}$ and the velocity field $\mathbf{u}$ are independent of $\mathbf{x}$, then the above commutator $\mathbf{E}_{1,2}$ equals zero, that is no splitting error occurs between advection and diffusion. A similar analysis leads to the following results. In the case

$$\nabla\mathbf{K} = 0, \quad \nabla\mathbf{u} = 0, \quad \nabla\sigma = 0, \quad \nabla\mathrm{E} = 0$$

any pair of the operators $\mathbf{F}_1$, $\mathbf{F}_2$, $\mathbf{F}_3$ and $\mathbf{F}_4$ L-commute, except for $\mathbf{F}_3$ and $\mathbf{F}_4$. Moreover, if the operator $\mathbf{F}_5$ is independent of $\mathbf{x}$, then it L-commutes with $\mathbf{F}_1$, and under some additional conditions with $\mathbf{F}_2$ and $\mathbf{F}_3$ as well. However, the operator $\mathbf{F}_4$ does not L-commute with the operators $\mathbf{F}_3$ and $\mathbf{F}_5$. (For details see *Dimov et al.* (1999).)

In practice the conditions for the non-existence of the splitting error are not usually satisfied. However, in certain meteorological situations they may be ap-

proximately satisfied. For example if the diffusion coefficient matrix **K** decreases to very small values (which is typical of night-time periods because of the increased stability of the atmosphere), the commutators between diffusion and advection and diffusion and chemistry strongly decrease, which presumably leads to a significant decrease of the splitting error.

In addition to the two different splitting procedures introduced in this chapter, other splittings can also be applied. We can divide the spatial differential operator into even more parts and obtain more systems that are even simpler. It is also possible to combine the splitting methods and apply different splittings over different time intervals. However, it is better to minimize the number of the splitted operators, because the splitting error is, as a rule, difficult to estimate.

8. Summary

Nowadays air pollution is one of the most urgent environmental problems, which necessitates the reliable modeling of the atmospheric transport of pollutants. Air pollution models are based on the (chemistry-)transport equations, a system of partial differential equations describing the concentration changes of the pollutants in the atmosphere due to several transport processes. This system can only be solved numerically.

In the paper first we introduce the transport equations, and then summarize the problems concerning the numerical solution of a system of partial differential equations in general. A reliable numerical method is expected to satisfy several requirements simultaneously also in the case of the transport equations. However, this system is so complicated that we cannot guarantee these important properties. In the paper we discuss a procedure which allows us to solve a few simpler systems instead of the whole one. This procedure is called operator splitting and is widely used in air pollution modeling, however, so far little investigation has been carried out into it. In the article we clarify the mathematical background and the role of operator splitting with the use of the Lie-algebra theory and give some examples of splitting procedures (DEM splitting, physical splitting).

When applying splitting in a mathematical model, it is important to know the error resulting from the splitting procedure itself, the so-called splitting error, which we also discuss in more details. We give some cases when this error vanishes, but in practical applicatons this rarely happens. Obviously, this error (together with the effect of other numerical errors) should be minimal. Therefore, it is important to analyse the splitting error of the applied schemes and possibly find others in which the error is even more reduced.

Acknowledgement—The authors are indebted to the referees for the valuable suggestions.

References

Brandt, J., Bastrup-Birk, A., Christensen, J. H., Mikkelsen, T., Thykier-Nielsen, S. and *Zlatev, Z.*, 1998: Testing the importance of accurate meteorological input fields and parameterizations in atmospheric transport modelling using DREAM - Validation against ETEX-1. *Atmospheric Environment 32*, 4167-4186.

Broecker, W.S., 1987: Unpleasant surprises in the greenhouse? *Nature 328*, 123-126.

Broecker, W. S., 1991: The great ocean conveyor. *Oceanography 4*, 79-89.

Crutzen, P.J. and *Zimmermann, P.H.*, 1991: The changing photochemistry of the troposphere. *Tellus 43A/B*:136.

Crutzen, P.J., 1995: Overview of tropospheric chemistry: Developments during the past quarter century and a look ahead. Faraday discussions 100:1.

Dimov, I., Faragó, I. and *Zlatev, Z.*, 1999: Commutativity of the operators in splitting methods for air pollution models. *Technical report 04/99.* Bulgarian Academy of Sciences.

Eliassen, A., Hov, O., Isaksen, J. S., Saltbones, J. and *Stordal, F.*, 1982: A Lagrangian long-range model with atmospheric boundary layer chemistry. *Journal of Applied Meteorology 21*, 1615-1661.

Engel, K.-J. and *Nagel, R.*, 2000: *One-Parameter Semigroups for Linear Evolution Equations.* Springer, New York.

Faragó, I., Hariton, H. A., Komáromi, N. and *Pfeil, T.*, 1993: The heat equation and the qualitative properties of its numerical solution I-II. Alkalmazott Matematikai Lapok 17, 101-141.

Houghton, J. T., Meira Filho, L. G., Callander, B. A., Harris, N., Kattenberg, A. and *Maskell, K.*, 1995: Climate Change 1995. The science of climate change. Published for the Intergovernmental Panel on Climate Change, Cambridge University Press, p. 572.

Keeling, C. D., Bacastow, R. B., Carter, I. F., Piper, S. C., Whorf, T. P., Heimann, M., Mook, W. G. and *Roeloffzen, H.*, 1989: A three-dimensional model of atmospheric CO_2 transport based on observed winds. 1. Analysis of observational data. *Geophis. Mono.*, Am. Geophys. Union, Washington, DC, 165-231.

Lanser, D. and *Verwer, J. G.*, 1999: Analysis of operator splitting for advection-diffusion-reaction problems in air pollution modelling. *J. Compute. Appl. Math. 111*, 201-216.

Marchuk, G. I., 1980: *Methods of Computational Mathematics* (in Russian). Nauka, Moscow.

Marchuk, G. I., 1988: *Methods of Splitting* (in Russian). Nauka, Moscow

Möller, D., 1999: Atmospheric environmental research. Critical decisions between technological progress and preservation of nature. Springer p. 185.

Olson, M. P., Bottenheim, J. W. and *Oikawa, K. K.*, 1992: Nitrogen source receptor matrices and model results for eastern Canada. *Atmospheric Environment 26A*, 2323-2340.

Piedelievre, J. P., Musson-Genon, L. and *Bompay, F.*, 1990: MEDIA - An Eulerian model of atmospheric dispersion, first validation on the Chernobyl release. *Journal of Applied Meteorology 29*, 1205-1220.

Simpson, D., 1992: Long-period modelling of photochemical oxidants in Europe. Model calculations for July 1985. *Atmospheric Environment 26A*, 1609-1634.

Simpson, D., 1993: Photochemical model calculations over Europe for two extended summer periods, 1985 and 1989. Model results and comparisons with observations. *Atmospheric Environment 27A*, 921-943.

Thomée, V., 1990: *Finite Difference Methods for Linear Parabolic Equations.* Elsevier, North-Holland.

Trenberth, K. E., 1992: *Climate System Modeling.* Cambridge University Press, 491-517.

Varadarajan, V. S., 1974: *Lie Groups, Lie Algebras and Their Representations.* Prentice-Hall, Inc., Englewood Cliffs, New Jersey.

Yanenko, N. N., 1962: On convergence of the splitting method for heat equation with variable coefficients (in Russian). *Journal of Comp. Math. and Math. Phys. 2.*

Zlatev, Z., 1995: *Computer Treatment of Large Air Pollution Models.* Kluwer Academic Publishers.

BOOK REVIEW

Warneck, P., 1999: **Chemistry of the Natural Atmosphere**. Academic Press, San Diego, San Francisco, New York, Boston, London, Sidney and Tokyo. 923 pages, a large quantity of tables, figures and supplementary tables with important data, a huge amount of references on 127 pages and a detailed index.

One of the milestones in the short history of atmospheric chemistry research was the publication of the book of *Christian E. Junge* in 1963 (*Air Chemistry and Radioactivity*) by the Academic Press in its famous International Geophysics Series. The present book is dedicated to the memory of the late professor Junge (1912–1996), "a pioneer in the exploration of atmospheric trace substances" and is written by a former Junge's associate. We have to note that the volume is worthy of the name of the late master. It can also be considered as a milestone in such a way that it summarizes in an excellent manner practically everything which has happened in this field during the last hundred fifty years, but mainly during the last part of the 20th century. In other words this book closes the first important time period of this field of atmospheric science. If the Junge's book announced the birth of a new branch of science, Warneck's book is a signal of its maturity.

Let us imagine that when the writer of the present review was a student, more than forty years ago, he learned at the University of Budapest that the atmosphere, beside oxygen, nitrogen and noble gases, contains as minor constituents only water vapor, carbon dioxide and "dusts" and that ozone is simply a substance which indicates the motion of atmospheric pressure systems, that is the mixing efficiency between the stratosphere and troposphere. Since that time we have understood that in the air we can find a lot of trace substances which are in a continuous chemical interactions with one another and water, that atmospheric oxygen level has a history and that the composition of the atmosphere is a consequence of a huge material flow in nature called biogeochemical cycles. Research in atmospheric chemistry has become more and more active due to the recognition that human activities influences the atmospheric composition including the acidity of atmospheric deposition ("acid rain") as well as ozone formation and removal in the stratosphere ("ozone hole") and troposphere ("smog"). For their results in this latter field three research workers (*P. Crutzen, M. Molina* and *F. S. Rowland*) were rewarded by Nobel price in 1995. This was the first Nobel price given for research in atmospheric science. During the last decades, owing to intensive studies in atmospheric physics and chemistry, we recognized that the burning of fossil fuels by man contributes significantly to the atmospheric greenhouse and man-made aerosol particles can modify not only

the cloud and precipitation formation, but also the solar radiation transfer, consequently the climate.

The reader can learn from Warneck's book the history and present state of our knowledge concerning the problems mentioned. At the same time the volume is prepared with a scientific deepness necessary for helping all young people who want to make research in this important field: its reading is an excellent and unavoidable starting point for any further activity in this field. On the other hand, it gives a good reference book for senior researchers specialized in a narrow sector of air chemistry. The content is divided in twelve chapters from basic concepts of the composition, structure and dynamics of the air to the evolution of the Earth's atmosphere. A chapter on photochemical processes and elementary reactions gives a good introduction of the subject for potential non-chemist readers. Further, we can find specialized chapters on the chemistry and cycle of ozone, organic species, as well as of nitrogen and sulfur compounds. One chapter is devoted to the discussion of the physics and chemistry of the atmospheric aerosol, an other one deals with the role of clouds and precipitation in the control of atmospheric pathways of other trace components. Last but not least, a chapter provides a good survey of the geochemistry of carbon dioxide. It should also be emphasized that the supplementary tables contain kinetic data of all possible chemical reactions in the atmosphere necessary for model calculations.

In the last years several books have been published on atmospheric chemistry. Without estimating the values of these books we note that the content and the deepness of the chapters reflect generally the interest of the author(s) which is rather understandable. If a book is good, for example, in atmospheric photochemistry, it is not too detailed concerning the atmospheric aerosol particles and clouds, and *vice versa*. The reviewer believes that even in this respect the present volume is unique: the author presents all the problems at the same high scientific level. Shortly, it is the best book on atmospheric chemistry published until now. Thus, it goes without saying that its reading is recommended to all present and future scientists interested in this young, but very attractive and promising field of atmospheric science.

E. Mészáros

ATMOSPHERIC ENVIRONMENT

an international journal

To promote the distribution of Atmospheric Environment *Időjárás* publishes regularly the contents of this important journal. For further information the interested reader is asked to contact *Prof. P. Brimblecombe*, School for Environmental Sciences, University of East Anglia, Norwich NR4 7TJ, U.K.; E-mail: atmos_env@uea.ac.uk

Volume 35 Number 1 2001

Short Communications

Volume 35 Number 2 2001

NOTES TO CONTRIBUTORS

The purpose of *Időjárás* is to publish papers in the field of theoretical and applied meteorology. These may be reports on new results of scientific investigations, critical review articles summarizing current problems in certain subject, or shorter contributions dealing with a specific question. Authors may be of any nationality but papers are published only in English.

Papers will be subjected to constructive criticism by unidentified referees.

* * *

The manuscript should meet the following formal requirements:

Title should contain the title of the paper, the names(s) of the author(s) with indication of the name and address of employment.

The title should be followed by an *abstract* containing the aim, method and conclusions of the scientific investigation. After the abstract, the *key-words* of the content of the paper must be given.

Three copies of the manuscript, typed with double space, should be sent to the Editor-in-Chief: *P.O. Box 39, H-1675 Budapest,* Hungary.

References: The text citation should contain the name(s) of the author(s) in Italic letter or underlined and the year of publication. In case of one author: *Miller* (1989), or if the name of the author cannot be fitted into the text: *(Miller,* 1989); in the case of two authors: *Gamov* and *Cleveland* (1973); if there are more than two authors: *Smith et al.* (1990). When referring to several papers published in the same year by the same author, the year of publication should be followed by letters a,b etc. At the end of the paper the list of references should be arranged alphabetically. For an article: the name(s) of author(s) in Italics or underlined, year, title of article, name of journal, volume number (the latter two in Italics or underlined) and pages. E.g. *Nathan, K. K.,* 1986: A note on the relationship between photosynthetically active radiation and cloud amount. *Időjárás 90,* 10-13. For a book: the name(s) of author(s), year, title of the book (all in Italics or underlined with except of the year), publisher and place of publication. E.g. *Junge, C. E.,* 1963: *Air Chemistry and Radioactivity.* Academic Press, New York and London.

Figures should be prepared entirely in black India ink upon transparent paper or copied by a good quality copier. A series of figures should be attached to each copy of the manuscript. The legends of figures should be given on a separate sheet. Photographs of good quality may be provided in black and white.

Tables should be marked by Arabic numbers and provided on separate sheets together with relevant captions. In one table the column number is maximum 13 if possible. One column should not contain more than five characters.

Mathematical formulas and *symbols:* non-Latin letters and hand-written marks should be explained by making marginal notes in pencil.

The final text should be submitted both in manuscript form and on *diskette.* Use standard 3.5" or 5.25" DOS formatted diskettes for this purpose. The following word processors are supported: WordPerfect 5.1, WordPerfect for Windows 5.1, Microsoft Word 5.5, Microsoft Word 6.0. In all other cases the preferred text format is ASCII.

* * *

Authors receive 30 *reprints* free of charge. Additional reprints may be ordered at the authors' expense when sending back the proofs to the Editorial Office.

Published by the Hungarian Meteorological Service

Budapest, Hungary

INDEX: 26 361

HU ISSN 0324-6329